New Phytologist

Research

Warming triggers stomatal opening by enhancement of photosynthesis and ensuing guard cell CO_2 sensing, whereas higher temperatures induce a photosynthesis-uncoupled response

Nattiwong Pankasem[1], Po-Kai Hsu[1], Bryn N. K. Lopez[1], Peter J. Franks[2] and Julian I. Schroeder[1]

[1]Cell and Developmental Biology Department, School of Biological Sciences, University of California San Diego, La Jolla, CA, 92093-0116, USA; [2]School of Life and Environmental Sciences, The University of Sydney, Sydney, NSW, 2006, Australia

Author for correspondence:
Julian I. Schroeder
Email: jischroeder@ucsd.edu

Received: *29 April 2024*
Accepted: *29 July 2024*

New Phytologist (2024) **244:** 1847–1863
doi: 10.1111/nph.20121

Key words: blue light, carbon dioxide, guard cell, heat stress, photosynthesis, protein kinase, stomata, heat.

Summary

- Plants integrate environmental stimuli to optimize photosynthesis vs water loss by controlling stomatal apertures. However, stomatal responses to temperature elevation and the underlying molecular genetic mechanisms remain less studied.
- We developed an approach for clamping leaf-to-air vapor pressure difference (VPD_{leaf}) to fixed values, and recorded robust reversible warming-induced stomatal opening in intact plants. We analyzed stomatal temperature responses of mutants impaired in guard cell signaling pathways for blue light, abscisic acid (ABA), CO_2, and the temperature-sensitive proteins, Phytochrome B (phyB) and EARLY-FLOWERING-3 (ELF3).
- We confirmed that *phot1-5/phot2-1* leaves lacking blue-light photoreceptors showed partially reduced warming-induced stomatal opening. Furthermore, ABA-biosynthesis, phyB, and ELF3 were not essential for the stomatal warming response. Strikingly, *Arabidopsis* (dicot) and *Brachypodium distachyon* (monocot) mutants lacking guard cell CO_2 sensors and signaling mechanisms, including *ht1*, *mpk12/mpk4-gc*, and *cbc1/cbc2* abolished the stomatal warming response, suggesting a conserved mechanism across diverse plant lineages. Moreover, warming rapidly stimulated photosynthesis, resulting in a reduction in intercellular (CO_2). Interestingly, further enhancing heat stress caused stomatal opening uncoupled from photosynthesis.
- We provide genetic and physiological evidence that the stomatal warming response is triggered by increased CO_2 assimilation and stomatal CO_2 sensing. Additionally, increasing heat stress functions via a distinct photosynthesis-uncoupled stomatal opening pathway.

Introduction

Stomata provide a gateway for plant CO_2 intake and water loss. The regulation of stomatal guard cell turgor and volume maintains plant water status, assists in evaporative cooling of leaves and canopies, and facilitates CO_2 influx for photosynthesis. Stomata achieve this through the sensing and integration of environmental signals, including blue light, red light, atmospheric CO_2 concentration, humidity, ozone, and pathogen-associated molecules (Merilo *et al.*, 2018; Matthews *et al.*, 2020; Clark *et al.*, 2022). Despite considerable progress toward understanding these signaling pathways, comparatively little is known about stomatal sensing and response to temperature changes.

The current average global surface temperature has risen 1.09°C higher in 2010–2020 compared with the preindustrial era (1850–1900) with a larger increase over land (1.59°C) and is projected to continue increasing through this century (IPCC, 2023). In light of this global warming, it is crucial to understand and predict how stomata will respond, as this has implications for the productivity and water use of crops and forests. Studies have shown that high temperatures can induce stomatal opening. One of the observations was in maize (Raschke, 1970). Several studies showed that stomatal apertures increased when exposed to elevated temperatures in *Vicia faba* (Rogers *et al.*, 1979) and in *Arabidopsis thaliana* (Kostaki *et al.*, 2020; Korte *et al.*, 2023). In *Vicia faba*, the accumulation of K^+ in stomatal guard cells (Rogers *et al.*, 1979) and increased activity of inward-rectifying K^+ channels in guard cell protoplasts (Ilan *et al.*, 1995) have been demonstrated and are consistent with temperature elevation-induced increased stomatal apertures.

Leaf mesophyll photosynthesis plays a pivotal role in regulating stomatal functions. Under red light, the elevation of CO_2 assimilation reduces the internal CO_2 concentration in leaves, contributing to the initiation of stomatal opening (Mott, 1988;

Roelfsema *et al.*, 2002). In addition, the accumulation of mesophyll-derived photosynthates and/or signals can affect stomatal movements in response to light and CO_2 (Lawson *et al.*, 2008; Mott *et al.*, 2008; Flütsch *et al.*, 2020).

Compared with microscopic stomatal aperture measurements in leaf epidermal peels, time-resolved gas exchange measurements of intact leaves or whole plants enable a larger signal-to-noise ratio, show time-dependent responses, and preserve intact communication between mesophyll and guard cells. Therefore, this approach has been widely used to quantify the kinetics of stomatal responses to blue light, CO_2, ozone, humidity, and small molecules. However, investigating temperature effects on stomatal conductance has been difficult because the stomatal temperature response can be confounded by stomatal sensitivity to the leaf-to-air vapor pressure difference (VPD_{leaf}). Increases in VPD_{leaf} cause stomatal closure (Running, 1976; Merilo *et al.*, 2018; Grossiord *et al.*, 2020; Hsu *et al.*, 2021), and temperature elevation will increase VPD_{leaf}. Therefore, studies seeking to measure stomatal sensitivity to temperature must control for sensitivity to VPD_{leaf} (e.g. maintain constant VPD_{leaf}).

A wealth of genetic resources in the model plant *Arabidopsis thaliana* enables the dissection of stomatal signaling mechanisms and pathways. Genetic mechanisms of environmental sensing and signal transduction in guard cells have been elucidated for several key stimuli. Stomatal opening is achieved by activating plasma membrane H^+-ATPases, causing plasma membrane hyperpolarization, which activates inward-rectifying K^+_{in} channels (Assmann *et al.*, 1985; Shimazaki *et al.*, 1986; Schroeder *et al.*, 1987; Pandey *et al.*, 2007), while deactivating anion channels (Marten *et al.*, 2007). Stomatal opening in response to blue light is regulated by two redundant blue light-sensing protein kinases, PHOTOTROPIN 1/2 (PHOT1/2) (Kinoshita *et al.*, 2001), a MAP4K kinase, BLUE LIGHT SIGNALING 1 (BLUS1) (Takemiya *et al.*, 2013), and two redundant Raf-like MAP3K kinase CONVERGENCE OF BLUE LIGHT AND CO_2 1 and 2 (CBC1/CBC2) (Hiyama *et al.*, 2017). Stomatal opening in response to low CO_2 is regulated by the CO_2/bicarbonate sensing protein kinase pair, HIGH TEMPERATURE 1 (HT1) and MITOGEN-ACTIVATED PROTEIN KINASE 12 and 4 (MPK12/MPK4), and HT1-mediated phosphorylation and activation of CBC1/CBC2 kinase activity (Takahashi *et al.*, 2022). Stomata close in response to endogenous ABA accumulated under abiotic stress conditions. Basal ABA levels correlate inversely with steady-state stomatal conductance in *Arabidopsis* ABA-deficient mutants (Merilo *et al.*, 2018). With regard to temperature signaling and response, Kostaki *et al.* (2020) found that increases in stomatal apertures at elevated temperatures of 35°C were reduced in *phot1/phot2* double mutant and H^+-ATPase-related mutants compared with wild-type (WT) controls. However, little else is known about the molecular genetic signal transduction mechanisms through which different degrees of elevated temperatures cause stomatal opening.

In this study, we improve gas exchange techniques to capture time-resolved changes in stomatal conductance in response to temperature increases and temperature reduction in intact leaves attached to intact plants while stabilizing the vapor pressure difference between leaves and ambient air. We investigated the hypotheses that temperature shift-induced changes in stomatal conductance may require guard cell signaling components and/or recently identified temperature-responsive proteins. *Arabidopsis thaliana* plants are relatively sensitive to temperature elevation, with growth being negatively impacted by temperatures above 27°C (Ludwig-Müller *et al.*, 2000) and 30°C (Sakata *et al.*, 2010). We systematically characterize the stomatal temperature response between 18°C and 28°C of defined key mutants impaired in blue light and CO_2/bicarbonate signal transduction mechanisms and ABA biosynthesis. In addition, we measured stomatal temperature responses of mutants that lack the direct temperature sensors, Phytochrome B (phyB) and EARLY FLOWERING 3 (ELF3), which are required for high temperature-induced changes in plant development (Legris *et al.*, 2016; Jung *et al.*, 2020). These analyses in many mutant backgrounds show a major role in temperature-dependent regulation of photosynthetic activity in leaves and the ensuing guard cell CO_2 signal transduction. We further develop and report an additional approach that allows time-resolved stomatal conductance recording of the temperature response upon elevation to 34°C in intact *Arabidopsis* plants, providing evidence that distinct mechanisms function at these two temperature ranges.

Materials and Methods

Plant materials and growth conditions

Arabidopsis thaliana (L.) Heynh. Columbia-0 (Col-0) ecotype, as WT, and mutant plants were grown in an autoclaved 3 : 1 Sunshine® Mix #1 (Sun Gro Horticulture, Alberta, Canada): vermiculite (PVP industry Inc., North Bloomfield, OH, USA) with 3.6 g l^{-1} of 14–14-14 slow-release fertilizer (Osmocote, Marysville, OH, USA). Seeds were stratified in the dark for 48 h at 4°C. *Arabidopsis* plants were grown under photosynthetic photon flux density of 100–150 µmol m^{-2} s^{-1} with a 10-h photoperiod, 22°C : 20°C, day : night temperatures, and 0.8–1 kPa saturation deficit in a growth chamber (Conviron, Manitoba, Canada). The *Brachypodium distachyon* (L.) P. Beauv. Bd21-3 line, as WT background, and *Bdmpk5* CRISPR mutant plants were grown in an autoclaved mixture of 3 : 1 : 1 Sunshine® Mix #1: perlite: vermiculite under photosynthetic photon flux density of 150–-200 µmol m^{-2} s^{-1} with a 16-h photoperiod, 22°C : 20°C, day : night temperatures, and 0.8–1 kPa vapor pressure deficit in a custom-made growth cabinet.

Arabidopsis and *Brachypodium* mutants investigated in this study were: *phyB-9* (Yoshida *et al.*, 2018), *nced3-2/nced5-2* (Frey *et al.*, 2012), *slac1-4/slah3-1/almt12-2* (Jalakas *et al.*, 2021), *ost1-3* (Yoshida *et al.*, 2002), *phot1-5/phot2-1* (Kinoshita *et al.*, 2001), *blus1-3* (Takemiya *et al.*, 2013), *ht1-2* (Hashimoto *et al.*, 2006), dominant *ht1-A109V* (Hõrak *et al.*, 2016), *cbc1/cbc2* (Hiyama *et al.*, 2017), two alleles of *mpk12/4-gc* (Tõldsepp *et al.*, 2018), and *Brachypodium Bdmpk5-crispr#3* mutant (Lopez *et al.*, 2024). Oligos used for genotyping by PCR or Sanger sequencing of these mutant loci are listed in Supporting Information (Table S1).

Time-resolved recordings of leaf gas exchange in response to temperature changes

We recorded gas exchange rates of intact leaves attached to 5- to 7-wk-old intact plants of Col-0 WT and mutants using a portable gas exchange analyzer (LI-6800-01A; Li-Cor Inc., Lincoln, NE, USA). Leaves were clamped into the leaf chamber and acclimated at 28°C leaf temperature, 400 µmol mol^{-1} CO_2, leaf-to-air vapor pressure difference (VPD_{leaf}) of 1.15–1.30 kPa, and 400 µmol s^{-1} of air flow rate for 60–120 min. *Arabidopsis* leaves were illuminated with 500 µmol m^{-2} s^{-1} photosynthetically active radiation (PAR) in the form of 9 : 1 red light (peak wavelength emission of 625 nm with a 16-nm full-width half-maximum bandwidth): blue light (peak wavelength emission of 475 nm with a 30-nm full-width half-maximum bandwidth) from the LED source of the LI-COR 6800-01A system. *Brachypodium* leaves were illuminated with 750 µmol m^{-2} s^{-1} using the same relative PAR spectra as above. After stomatal conductance to water vapor (g_{sw}) readings were stable, gas exchange readings were recorded every 30 s for 180 min. Unless indicated otherwise, the baseline gas exchange rates were logged at 28°C for 30 min, followed by cooling down at 0.5°C min^{-1} and maintained at 18°C of leaf temperature for a total of 60 min. The leaf temperature was then increased at 2°C min^{-1} and kept at 28°C for a total of 90 min. This sequence was repeated in separate experiments as described in figure legends for leaves exposed to 150 µmol m^{-2} s^{-1} of the identical relative PAR spectra described above, as well as darkness. When the same controls were recorded within a set of experiments on different genotypes, the same control experiments are shown in the corresponding figures for these genotypes. Because VPD_{leaf} is affected by temperature and stomata are sensitive to VPD_{leaf}, we maintained VPD_{leaf} at 1.15–1.3 kPa throughout the measurements. The stomatal conductance (g_{sw}) was not plotted during the first 25 min of temperature decrease and 15 min of temperature elevation due to unstable readings of water vapor concentration, as described in the Results section. The same 6800-01A LI-COR gas exchange analyzer was used for all experiments reported here. Offsets between the two internal infrared gas analyzers reading reference air and sample air within the 6800-01A LI-COR integrated gas exchange analyzer system were corrected according to the manufacturer's instruction by the range match functions spanning 0 to 2200 µmol mol^{-1} and 2 to 28 mmol mol^{-1} of reference CO_2 and water vapor concentrations, respectively.

For experiments analyzing responses up to 34°C, leaves were clamped into the leaf chamber and acclimated at 34°C, 400 µmol mol^{-1} CO_2, leaf-to-air vapor pressure difference (VPD_{leaf}) of 1.5 kPa, and 250 µmol s^{-1} of air flow rate for 60–120 min. Leaves were illuminated with 150 µmol m^{-2} s^{-1} PAR in a 9 : 1 red light: blue light ratio. To maintain VPD_{leaf}, the gas exchange analyzer and plant were exposed to a high ambient temperature of 29°C for 4.5 h. inside the growth chamber. After stomatal conductance (g_{sw}) readings were stable, stomatal conductance and CO_2 assimilation rate readings were recorded every 30 s for 180 min. The baseline gas exchange rates were logged at 34°C for 30 min, followed by cooling down at 0.6°C min^{-1} and maintained at 22°C of leaf temperature for a total of 60 min. The leaf temperature was then increased at 0.6°C min^{-1} and kept at 34°C for a total of 90 min.

The difference of g_{sw} (Δg_{sw}) of individual measurements was calculated by subtracting the average of 5-min recordings at 25.5–30.0 min (30 min), 65.5–70.0 min (70 min), 85.5–90.0 min (90 min), 115.5–120.0 min (120 min), and 175.0–179.5 min (180 min). Half-time responses for stomatal closing and opening were calculated as the time required to achieve 50% of the recorded maximum stomatal conductance reduction and 50% of the recorded maximum stomatal conductance increase, respectively.

Leaf photosynthesis measurements

Leaves of Col-0 WT plant were acclimated for 5–10 min at the indicated light fluence rates and/or leaf temperatures. Then, net CO_2 assimilation rates (A) and leaf intercellular CO_2 concentrations (c_i) were recorded at 12 sequential reference CO_2 concentrations from 400, 300, 200, 100, 50, 25, 400, 600, 800, 1000, 1300, and 1500 µmol mol^{-1}. To derive the maximum rate of carboxylation ($V_{c_{max}}$) and the rate of electron transport (J), CO_2 assimilation rates as a function of the c_i were analyzed with the Farquhar–von Caemmerer–Berry model (Farquhar *et al.*, 1980) using the Plantecophys package in R (Duursma, 2015).

Results

Intact plants show robust and reversible changes in stomatal conductance in response to temperature shifts

To investigate the effect of temperature changes on stomatal movements in intact plants, we developed time-resolved gas exchange measurements in intact leaves to capture the stomatal response to temperature shifts. Under water-unsaturated air, changing leaf temperature causes an increased VPD_{leaf}. High VPD_{leaf} is the driving force of evapotranspiration and induces stomatal closure (Running, 1976; Merilo *et al.*, 2018; Grossiord *et al.*, 2020). In this study, we maintained the VPD_{leaf} at a stable level by adjusting the incoming water vapor concentration while temperature changes were imposed. We observed a time-resolved reduction in stomatal conductance in Col-0 WT leaves in response to temperature decreases from 28°C to 18°C (Fig. 1a; Paired Student's t-test, $P = 0.016$ from 30 min at 28°C to 70 min at 18°C, $P = 0.021$ from 30 min at 28°C to 90 min at 18°C). Temperature elevation from 18°C to 28°C resulted in increases in stomatal conductance (Fig. 1b; $P = 0.005$ from 90 min at 18°C to 120 min at 28°C, $P = 0.022$ from 90 min at 18°C to 180 min at 28°C; paired Student's t-test). We measured stomatal responses to temperature shifts and found consistent results in >10 sets of independent experiments ($n = 3$–9 Col-0 WT leaves for each independent set of experiments). Note that initially, during the imposed temperature shifts, VPD_{leaf} control showed slight instability while the LI-6800-01A made the necessary internal adjustments (Fig. 1c), and these brief periods were, therefore, not included in the analyses. During these initial

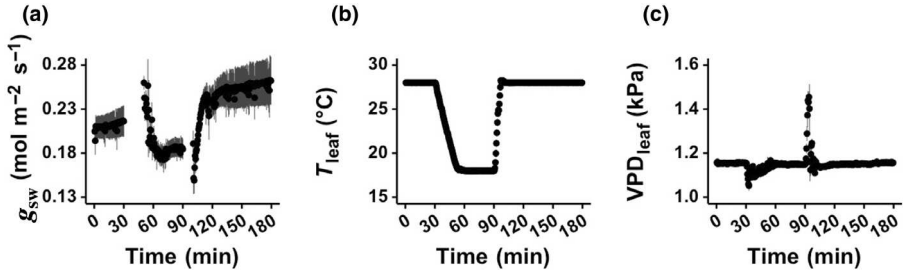

Fig. 1 Stomatal conductance (g_{sw}) of Col-0 wild-type (WT) changes reversibly in response to temperature changes. (a) Time-resolved stomatal conductance (g_{sw}) changes in response to (b) leaf temperature (T_{leaf}) shifts in Col-0 WT leaves ($n = 4$) while (c) the leaf-to-air vapor pressure difference (VPD_{leaf}) was maintained. Measurements were performed under 450 µmol m^{-2} s^{-1} of red light combined with 50 µmol m^{-2} s^{-1} of blue light, a CO_2 concentration of 400 µmol mol^{-1}, and *c*. 1.2 kPa leaf-to-air vapor pressure difference. Records of stomatal conductance are not shown immediately during the temperature transition (See the Results and Materials and Methods sections). Note that the same Col-0 WT data are shown in Fig. 5(a–c, g–i), Supporting Information Fig. S11(a–d), as those mutants were grown in parallel and measured in the same set of experiments. Data represent mean ± SE. Col-0 WT leaves were measured in >10 sets of independent experiments; each showed similar findings.

periods, stomatal conductance could show responses opposite to the temperature effects (Fig. 1a). These transient responses are in line with an initial VPD_{leaf} response before the VPD_{leaf} was stabilized (Fig. 1c). We leveraged these techniques to investigate the genetic requirement of key guard cell signaling components for the stomatal temperature response.

Anion channels and OST1/SnRK2.6 kinase are genetically required for stomatal responses to temperature shifts

Slow-type and rapid-type anion channels in the plasma membrane are central to guard cell osmotic regulation (Keller *et al*., 1989; Schroeder & Hagiwara, 1989; Schroeder *et al*., 1993; Negi *et al*., 2008; Vahisalu *et al*., 2008; Meyer *et al*., 2010). We tested the stomatal temperature response of *slac1/slah3/almt12* triple-mutant leaves disrupting the S-type anion channels (*SLOW ANION CHANNEL-ASSOCIATED 1; SLAC1* and *SLAC1 HOMOLOG 3; SLAH3*) and R-type anion channel (-*ALUMINUM-ACTIVATED, MALATE TRANSPORTER 12; ALMT12*). We found that *slac1-4/slah3-1/almt12-2* triple-mutant leaves have a significantly higher steady-state stomatal conductance than Col-0 WT (Fig. S1a). Upon decreasing the temperature from 28°C to 18°C, the stomatal conductance of the triple mutant decreased slightly and continued to decrease slowly until the end of low-temperature exposures (Fig. S1a). Strikingly, we found that the stomatal conductance of *slac1-4/slah3-1/almt12-2* triple-mutant leaves did not increase when shifting the temperature from 18°C to 28°C (Fig. S1a,c). The high stomatal conductance in *slac1-4/slah3-1/almt12-2* triple-mutant leaves may be a cause for the lack of further opening. The limited stomatal responses to temperature changes indicate that S-type and R-type anion channels play a role in stomatal responses to temperature changes (Fig. S1).

OPEN STOMATA1/SUCROSE-NON-FERMENTING-1-RELATED 2.6 (OST1/SnRK2.6) is a member of the SnRK2 protein kinase family in *Arabidopsis*. OST1/SnRK2.6 function is central for stomatal closure at post-translational and transcriptional levels (Mustilli *et al*., 2002). High ABA concentrations in guard cells inhibit group A type 2C protein phosphatase, activating OST1 kinase activity (Ma *et al*., 2009; Park *et al*., 2009). OST1, in turn, activates SLAC1 through phosphorylation and causes anion efflux and, thus, stomatal closure (Geiger *et al*., 2009; Lee *et al*., 2009; Brandt *et al*., 2012), and *ost1-3* mutants impair multiple stomatal closing responses. We measured stomatal conductance in response to temperature shifts of the *ost1-3* mutant leaves. We found that *ost1-3* mutant leaves show high steady-state stomatal conductance, a delayed stomatal closing in response to temperature reduction compared with Col-0 WT, and no clear stomatal opening in response to temperature elevation (Fig. S2), indicating that OST1/SnRK2.6 function is important for the stomatal temperature response.

Analyses of blue-light signaling mutants in warming-induced stomatal opening

Blue light receptors PHOT1/2 and the downstream BLUS1 kinase are required for stomatal opening in response to blue light (Kinoshita *et al*., 2001; Takemiya *et al*., 2013) We found that stomatal closure of *phot1-5/phot2-1* double-mutant leaves in response to temperature reduction occurred. Warming-induced steady-state stomatal opening in *phot1-5/phot2-1* double-mutant leaves was significantly reduced in two sets of independent experiments (Fig. 2a–c: $P = 0.046$ from 90 min at 18°C to 120 min at 28°C, $P = 0.044$ from 90 min at 18°C to 150 min at 28°C; $n = 4$ plants per genotype and Fig. S3(a–c); $P = 0.193$ from 90 min at 18°C to 120 min at 28°C, $P = 0.005$ from 90 min at 18°C to 150 min at 28°C; $n = 4$ plants per genotype; one-way ANOVA with *post hoc* Tukey's HSD test). We investigated whether the downstream BLUS1 kinase is genetically necessary. We found that *blus1-3* mutant leaves disrupting the BLUS1 kinase (Takemiya *et al*., 2013) showed robust steady-state stomatal closing in response to temperature reduction with some slight difference in the initial response in one set of experiments (Fig. 2a,b: $P = 0.044$ from 30 min at 28°C to 70 min at 18°C, $P = 0.110$ from 30 min at 28°C to 90 min at 18°C; $n = 6$ plants per genotype; independent Students' *t*-test and Fig. S3(a,b);

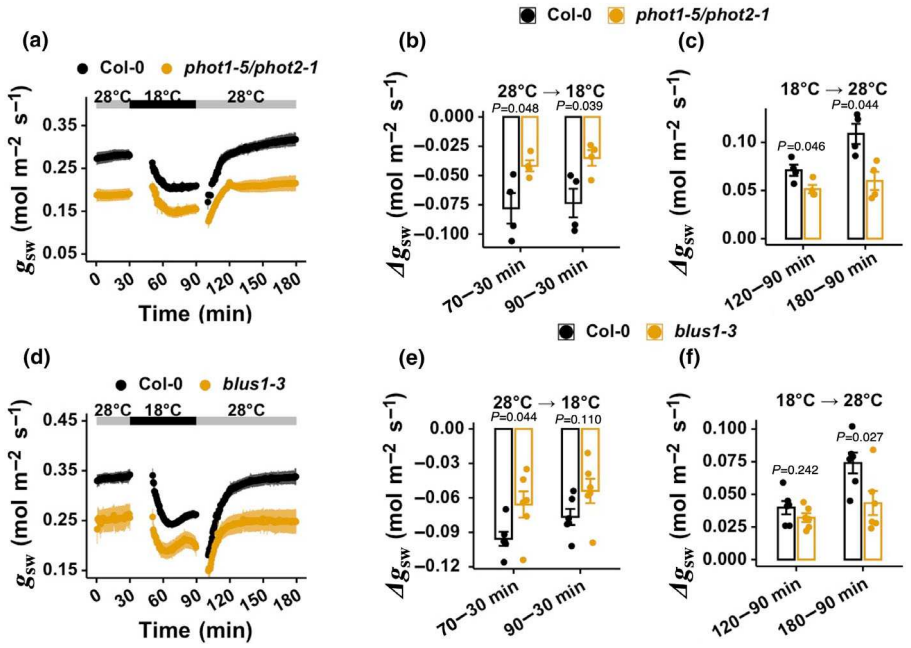

Fig. 2 Stomatal blue light signaling partially contributes to warming-induced stomatal opening (a, d) Time-resolved stomatal conductance (g_{sw}) changes in response to temperature changes in leaves of Col-0 wild-type (WT) ($n = 4$), the *phot1-5/phot2-1* double mutant ($n = 4$) in (a), and the *blus1-3* mutant ($n = 6$) in (d). Measurements were performed under 450 μmol m^{-2} s^{-1} of red light combined with 50 μmol m^{-2} s^{-1} of blue light, a CO_2 concentration of 400 μmol mol^{-1}, and *c*. 1.2 kPa of leaf-to-air vapor pressure difference. (b, c, e, f) Changes in stomatal conductance (Δg_{sw}) in response to temperature decreases in (b, e) and temperature increases in (c, f) were determined as described in the Materials and Methods section. Note that the same Col-0 WT control data are shown in Fig. 2(a–c), Supporting Information Fig. S5(a–c) as other mutants were grown in parallel and measured in the same set of experiments. Data represent mean ± SE. Statistical analyses in (b, c) were done using one-way ANOVA with pairwise Tukey's HSD *post hoc* test between the WT and the mutant line; the *P*-values presented above bar graphs are the same as in Fig. S16(a–d). For (e–f), statistical analyses were done using independent Student's *t*-tests between the WT and the mutant line. *phot1-5/phot2-1* double-mutant and *blus1-3* mutant leaves were measured in another set of independent experiments as shown in Fig. S3(a–f), respectively.

$P = 0.660$ from 30 min at 28°C to 70 min at 18°C, $P = 0.550$ from 30 min at 28°C to 90 min at 18°C; $n = 4$ plants per genotype; one-way ANOVA with *post hoc* Tukey's HSD test). In addition, stomatal conductance of *blus1-3* mutant leaves increased in response to the imposed temperature increase with a reduced steady-state response in one set of experiments compared with Col-0 WT (Fig. 2d–f: $P = 0.242$ from 90 min at 18°C to 120 min at 28°C, $P = 0.027$ from 90 min at 18°C to 150 min at 28°C; $n = 6$ plants per genotype and Fig. S3(d–f); $P = 0.173$ from 90 min at 18°C to 120 min at 28°C, $P = 0.975$ from 90 min at 18°C to 150 min at 28°C; $n = 4$ plants per genotype; one-way ANOVA with *post hoc* Tukey's HSD test).

De novo synthesis of ABA is not essential for stomatal closure in response to temperature reduction from 28°C to 18°C

Reduced stomatal conductance is associated with elevated leaf ABA concentrations. Therefore, we investigated whether *de novo* synthesis of ABA by NINE-*CIS*-EPOXYCAROTENOID DIOXYGENASE 3/5 (NCED3/NCED5) proteins is involved in stomatal closure in response to temperature reduction. We measured the stomatal conductance of *nced3-2/nced5-2* double mutant, impairing the rate-limiting NCED3/NCED5 enzymes for ABA synthesis, which results in low ABA levels in leaves (Iuchi *et al.*, 2001; Chater *et al.*, 2015; Hsu *et al.*, 2018). As expected, *nced3-2/nced5-2* double-mutant leaves showed a high steady-state stomatal conductance (Fig. S4a). Interestingly, stomatal conductance robustly and significantly decreased in response to temperature decreases and even showed a slightly higher average decrease in steady-state stomatal conductance than parallel-grown WT control plants (Fig. S4b). In contrast to the high stomatal conductance of *slac1-4/slah3-1/almt12-2* triple mutant (Fig. S1c) and *ost1-3* mutant (Fig. S2c,f), the stomatal conductance of *nced3-2/nced5-2* double-mutant leaves rose in response to temperature elevation similar to WT control plants (Fig. S4a–c). Since reduced ABA levels in *nced3/nced5* double-mutant impair stomatal closing in response to other stimuli but did not reduce the cooling-induced stomatal closing response (Fig. S4), these data suggest that *de novo* synthesis of stress-linked ABA is not essential for the stomatal closing response to temperature decreases.

phyB-9 and *elf3-1* mutants disrupting temperature sensing do not show a dramatic effect on stomatal temperature response

Plant development at temperatures greater than 25–27°C is regulated by direct biophysical changes associated with transcriptional

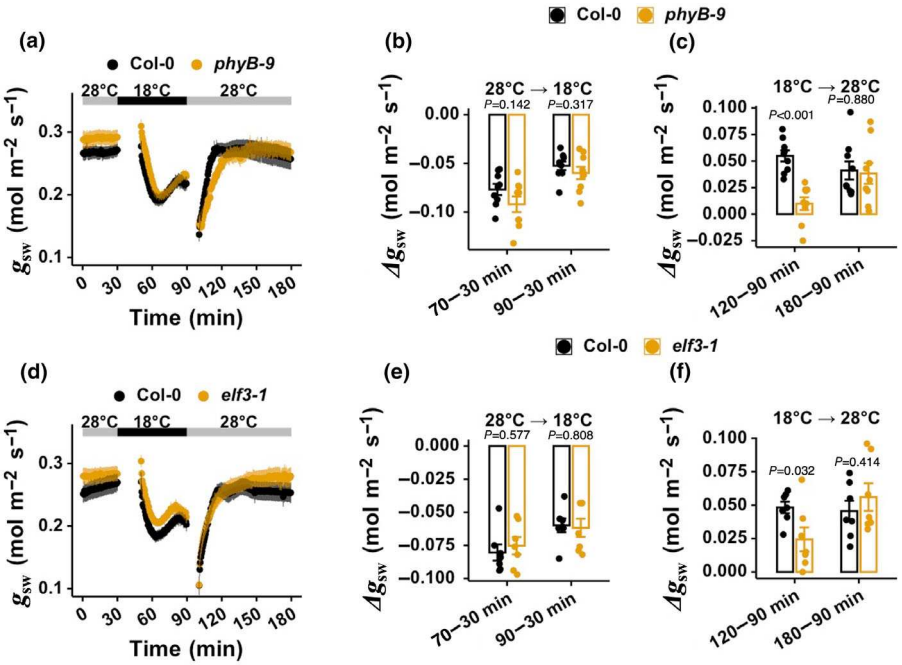

Fig. 3 *phyB-9* mutant and *elf3-1* mutant do not show a dramatic effect on stomatal responses to temperature changes. (a, d) Time-resolved stomatal conductance (g_{sw}) changes in response to temperature in leaves of Col-0 wild-type (WT) ($n = 7$–9), *phyB-9* mutant ($n = 9$) in (a), and *elf3-1* mutant ($n = 7$) in (d). Measurements were performed under 450 μmol m^{-2} s^{-1} of red light combined with 50 μmol m^{-2} s^{-1} of blue light, a CO_2 concentration of 400 μmol mol^{-1}, and *c.* 1.2 kPa of leaf-to-air vapor pressure difference. (b, c, e, f) Changes in stomatal conductance (Δg_{sw}) in response to temperature decreases in (b, e) and temperature increases in (c, f) were determined as described in the Materials and Methods section. Data represent mean ± SE. Statistical analyses were done using independent Student's *t*-tests between the WT and the mutant line; the *P*-values are presented above bar graphs (see also Supporting Information Fig. S12). *phyB-9* and *elf3-1* mutant leaves were measured in another set of independent experiments as shown in Fig. S5(a–f).

responses conferred by the thermal reversion of inactive to active forms of phyB (Legris *et al.*, 2016) and condensate formation of EARLY-FLOWERING 3 containing a temperature-sensitive prion-like domain (Jung *et al.*, 2020). In publicly available transcriptome datasets, both *phyB* and *ELF3* express at moderate to high levels in mature guard cells (Yang *et al.*, 2008; Pandey *et al.*, 2010; Bates *et al.*, 2012). It is possible that these known plant temperature sensors may be essential for stomatal responses to elevated temperatures. We tested this hypothesis by measuring the stomatal conductance of the strong *phyB-9* mutant allele that disrupts phyB function (Reed *et al.*, 1993; Yoshida *et al.*, 2018) and the *elf3-1* mutant lacking ELF3 functions (Covington *et al.*, 2001). *phyB-9* mutant leaves exhibited similar steady-state stomatal conductance responses to temperature reduction as WT controls but showed a reduction in stomatal opening at an early time point, which was consistent in two set of independent experiments (Fig. 3a–c; $P < 0.001$ from 90 min at 18°C to 120 min at 28°C, $P = 0.880$ from 90 min at 18°C to 180 min at 28°C; $n = 9$ plants per genotype; independent Students' *t*-test and Fig. S5a; $P = 0.001$ from 90 min at 18°C to 120 min at 28°C, $P = 0.168$ from 90 min at 18°C to 180 min at 28°C; $n = 4$ plants per genotype; one-way ANOVA with *post hoc* Tukey's HSD test). These data show a slight effect in *phyB* mutant leaves, but phyB is not essential for the steady-state temperature increase response. Similarly, *elf3-1* mutant leaves showed a slight difference in stomatal conductance responses to temperature elevation, which was consistent with two sets of independent experiments (Fig. 3d–f; $P = 0.032$ from 90 min at 18°C to 120 min at 28°C, $P = 0.414$ from 90 min at 18°C to 180 min at 28°C; $n = 7$ plants per genotype and Fig. S5d–f; $P = 0.025$ from 90 min at 18°C to 120 min at 28°C, $P = 0.080$ from 90 min at 18°C to 180 min at 28°C; $n = 4$ plants per genotype; independent Students' *t*-test). ELF3 may slightly affect the stomatal temperature response but is not essential for the steady-state stomatal temperature responses.

Stomatal CO_2/bicarbonate sensing and signaling mechanisms are essential for stomatal temperature responses

Elevated CO_2 concentrations induce stomatal closure, and reduced CO_2 concentrations cause stomatal opening. Recently, a high CO_2/bicarbonate-dependent inhibitory interaction of the Raf-like protein kinase HT1 with the MPK12/MPK4 was identified as a biochemical mechanism for the primary CO_2/bicarbonate sensor in guard cells (Takahashi *et al.*, 2022). Here, we measured stomatal temperature responses of *ht1-2* mutant leaves. The *ht1-2* mutant, which strongly impairs HT1 kinase activity, displays constitutively low stomatal conductance and fails to open stomata in response to low CO_2 concentration (Hashimoto *et al.*, 2006). Strikingly, we found that stomatal closing in response to temperature reduction and stomatal opening in response to temperature warming were severely impaired in *ht1-2* mutant leaves (Figs 4a–c, S6a–c).

Next, we tested the stomatal temperature response of a dominant *ht1*-A109V mutant allele in the *HT1* gene (Hõrak *et al.*, 2016). The HT1-A109V mutation is linked to the disruption of the inhibitory interaction of HT1 with MPK12 or MPK4 (Takahashi *et al.*, 2022) and, therefore, causes a constitutively high stomatal conductance and defective stomatal closure in response to elevated CO_2 (Hõrak *et al.*, 2016). Interestingly, we found that *ht1-A109V* mutant leaves showed dramatic

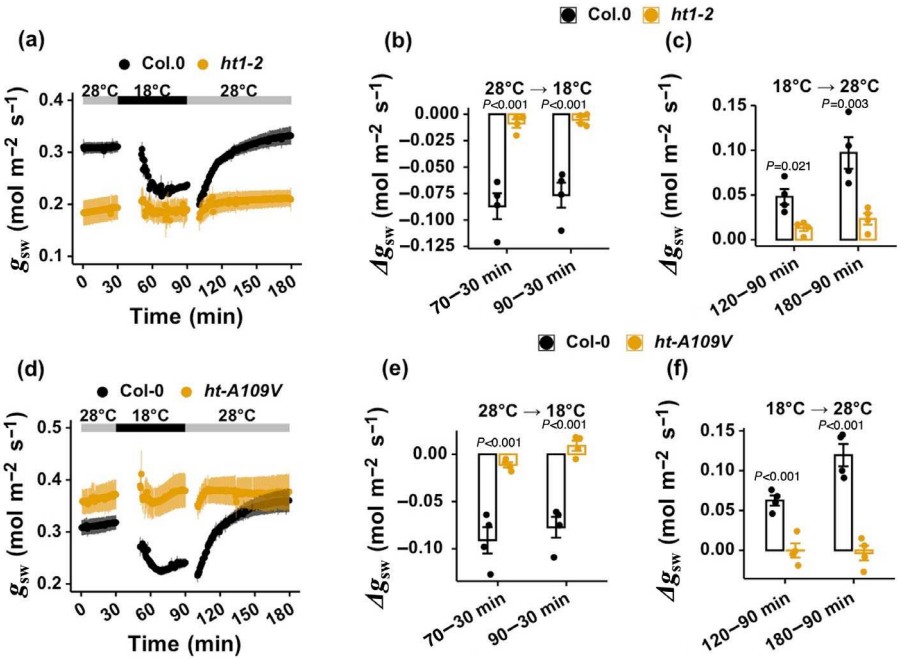

Fig. 4 Stomatal responses to temperature shifts are severely impaired in CO_2/bicarbonate sensing *ht1-2* and dominant *ht1-A109V* mutant leaves. (a, d) Time-resolved stomatal conductance (g_{sw}) changes in response to temperature changes in leaves of Col-0 wild-type (WT) and *ht1-2* mutant ($n = 4$) in (a) and *ht1-A109V* mutant ($n = 4$) in (d). Measurements were performed under 450 µmol m^{-2} s^{-1} of red light combined with 50 µmol m^{-2} s^{-1} of blue light, a CO_2 concentration of 400 µmol mol^{-1}, and *c*. 1.2 kPa of leaf-to-air vapor pressure difference. (b, c, e, f) Changes in stomatal conductance (Δg_{sw}) in response to temperature decreases in (b, e) and temperature increases in (c, f) were determined as described in the Materials and Methods section. Note that the same Col-0 WT control data are shown in (a–c) are the same as shown in Fig. 6(a–c), while the control data in (d–f) are similar to Fig. 7(a–c), Supporting Information Figs S2(d–f), S4(a–c), as other mutants were grown in parallel and measured in the same sets of experiments. Data represent mean ± SE. Statistical analyses were done using one-way ANOVA with pairwise Tukey's HSD *post hoc* test between the WT and the mutant line; the *P*-values presented above bar graphs are the same as in Figs S13(a–d) and S14(a–d) for *ht1-2* mutant and *ht1-A109V* mutant. The *ht1-2* mutant and *ht1-A109V* mutant leaves were measured in another set of independent experiments as shown in Fig. S6(a–f), respectively.

impairments in stomatal conductance changes in response to temperature shifts in contrast to WT controls (Figs 4d–f, S6d–f).

In further experiments, we measured the stomatal temperature responses in two independent lines of *mpk12/mpk4-gc* double mutants associated with loss of MPK12 function and reduced expression levels of *MPK4* in guard cells (Tõldsepp *et al.*, 2018). We found that *mpk12/mpk4-gc* double-mutant leaves had higher steady-state stomatal conductances, as expected, and either failed to respond or showed a weak response to temperature changes (Figs 5a–c, S7a–c). The statistical variability and larger confidence interval in the stomatal opening response found for the *mpk12/4-gc-1* allele (Fig. 5c; $P = 0.210$ from 90 min at 18°C to 180 min at 28°C; one-way ANOVA with *post hoc* Tukey's HSD test) may be due to the less perfect silencing of *mpk4* in guard cells in this propagated line. In *Brachypodium distachyon*, a single *BdMPK5* gene was identified as an *Arabidopsis MPK12/MPK4* ortholog by forward genetic screening (Lopez *et al.*, 2024). Therefore, full knockout of the orthologous *BdMPK5* gene is feasible in *Brachypodium* (Lopez *et al.*, 2024). We thus tested *Bdmpk5* CRISPR knockout mutant plants and compared the responses with the response of the Bd21-3 WT parent line. These experiments showed that *Bdmpk5* mutant leaves show only a weak stomatal closing response to temperature reduction and an absence of warming-induced stomatal opening (Fig. 5d–f).

CONVERGENCE OF BLUE LIGHT AND CO_2 1 and 2 are Raf-like kinases that function downstream of HT1 and the blue light sensor PHOT1 (Hiyama *et al.*, 2017). CBC1 is required for the blue light inhibition of the S-type anion channel activity and for stomatal opening in response to low CO_2 and blue light exposure (Hiyama *et al.*, 2017). In addition to the CO_2/bicarbonate sensor components, HT1 and MPK12/4, we tested whether the directly downstream located CBC1 and CBC2 (Hiyama *et al.*, 2017; Takahashi *et al.*, 2022) are required for stomatal temperature responses. We measured the changes in stomatal conductance of *cbc1/cbc2* double-mutant leaves. Similar to the *ht1-2* kinase mutant, *cbc1/cbc2* double-mutant leaves showed strongly impaired stomatal responses to temperature shifts (Figs 5g–i, S7d–f). Notably, together, the impaired stomatal temperature response phenotypes of *ht1-2* mutant, *ht1-A109V* mutant, *mpk12/4-gc* double mutants, and *cbc1/cbc2* double-mutants point to the model that guard cell CO_2/bicarbonate sensing and signaling mechanisms are essential for stomatal temperature warming responses in the investigated range. However, the underlying mechanisms remained unclear.

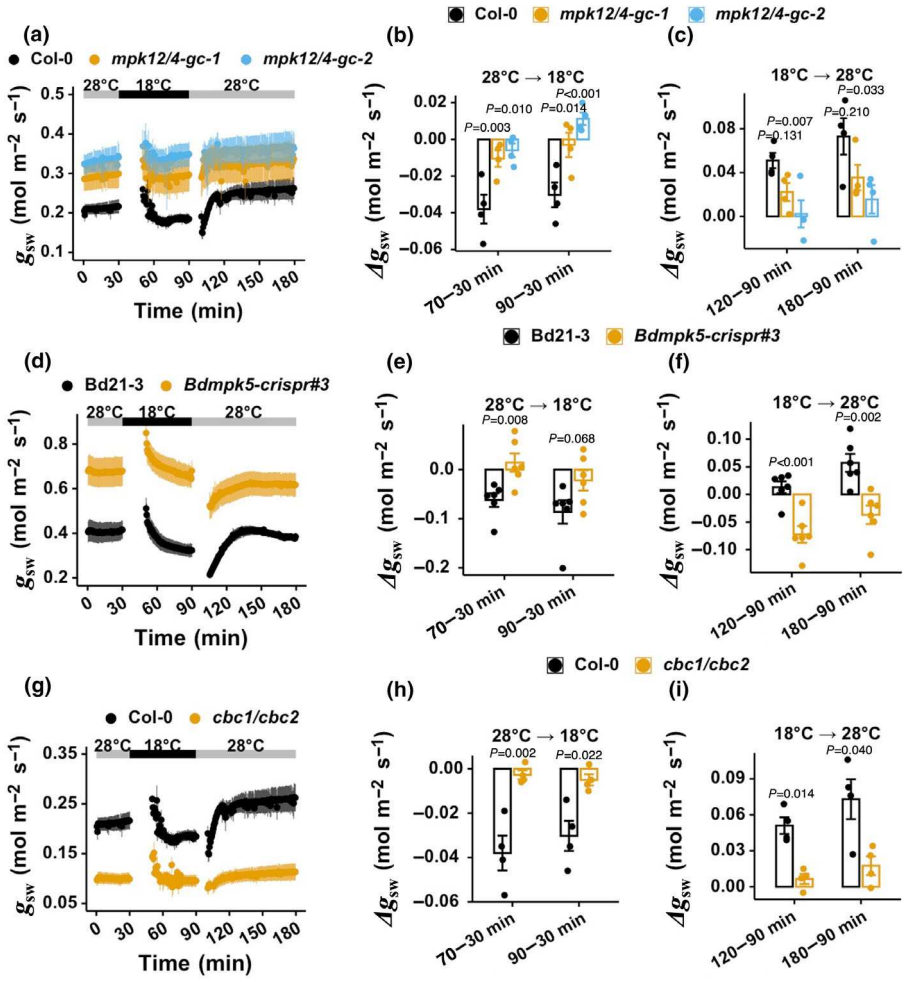

Fig. 5 Impaired temperature shift-induced stomatal conductance responses of *Arabidopsis mpk12/mpk4-gc* double mutant, *Brachypodium Bdmpk5 mutant*, and *cbc1/cbc2* double-mutant leaves. (a, d, g) Time-resolved stomatal conductance (g_{sw}) changes in response to temperature changes in leaves of Col-0 wild-type (WT) (a, g, $n = 4$), *Brachypodium* Bd21-3 WT (d, $n = 6$ plants), *mpk12/4-gc* mutant leaves ($n = 4$) in (a), *Brachypodium Bdmpk5* mutant (d, $n = 6$ plants) and *cbc1/cbc2* double-mutant leaves ($n = 4$) in (g). For *Arabidopsis* experiments in (a–c) and (g–i), measurements were performed under 450 μmol m^{-2} s^{-1} of red light combined with 50 μmol m^{-2} s^{-1} of blue light, a CO_2 concentration of 400 μmol mol^{-1}, and *c.* 1.2 kPa of leaf-to-air vapor pressure difference. Measurements in experiments in (d–f) were conducted similarly, except *Brachypodium* leaves were illuminated under 675 μmol m^{-2} s^{-1} of red light combined with 75 μmol m^{-2} s^{-1} of blue light. (b, c, e, f, h, i) Changes in stomatal conductance (Δg_{sw}) in response to temperature decreases in (b, e, h) and temperature increases in (c, f, i) were determined as described in the Materials and Methods section. Note that the same *Arabidopsis* Col-0 WT control data are shown in Fig. 5(a–c, g–i), as other mutants were grown in parallel and measured in the same set of experiments. Data represent mean ± SE. For (b, c) and (h, i), statistical analyses were done using one-way ANOVA with pairwise Tukey's HSD *post hoc* test between the *Arabidopsis* Col-0 WT and the mutant line; the *P*-values presented above bar graphs are the same as in Fig. S11(a–d). For (e–f), statistical analyses were performed using independent Student's *t*-tests between the Bd21-3 WT and the mutant line. The *Arabidopsis mpk12/4-gc-2* double mutant and *cbc1/cbc2* double-mutant leaves were measured in another set of independent experiments as shown in Fig. S7(a–f), respectively.

Stomatal temperature response is dependent on light intensity

We observed robust stomatal temperature responses when measured at a high light intensity of 500 μmol m^{-2} s^{-1} in Col-0 WT controls. Strikingly, a clear steady-state stomatal temperature response was absent under a low light fluence rate of 150 μmol m^{-2} s^{-1} (Fig. 6a–c; wild-type at low light: $P = 0.410$ from 30 min at 28°C to 90 min at 18°C, and $P = 0.634$ from 90 min at 18°C to 180 min at 28°C; Paired Student's *t*-test and Fig. S8a–c). The warming-induced increase in stomatal conductance under high light was associated with rapidly increased CO_2 assimilation rates (Figs 6d–f, S8d–f). Under high light at 28°C, an increased CO_2 assimilation was confirmed with increases in maximum carboxylation efficiency ($V_{c_{max}}$) and electron transport rate (J) (Fig. 6g–j).

To test the hypothesis that increased photosynthesis is required for the stomatal temperature response, we measured stomatal conductance in response to temperature changes under darkness. We found that the stomatal temperature response was disrupted in the dark when photosynthesis was absent (Figs 7a–c, S9a–c).

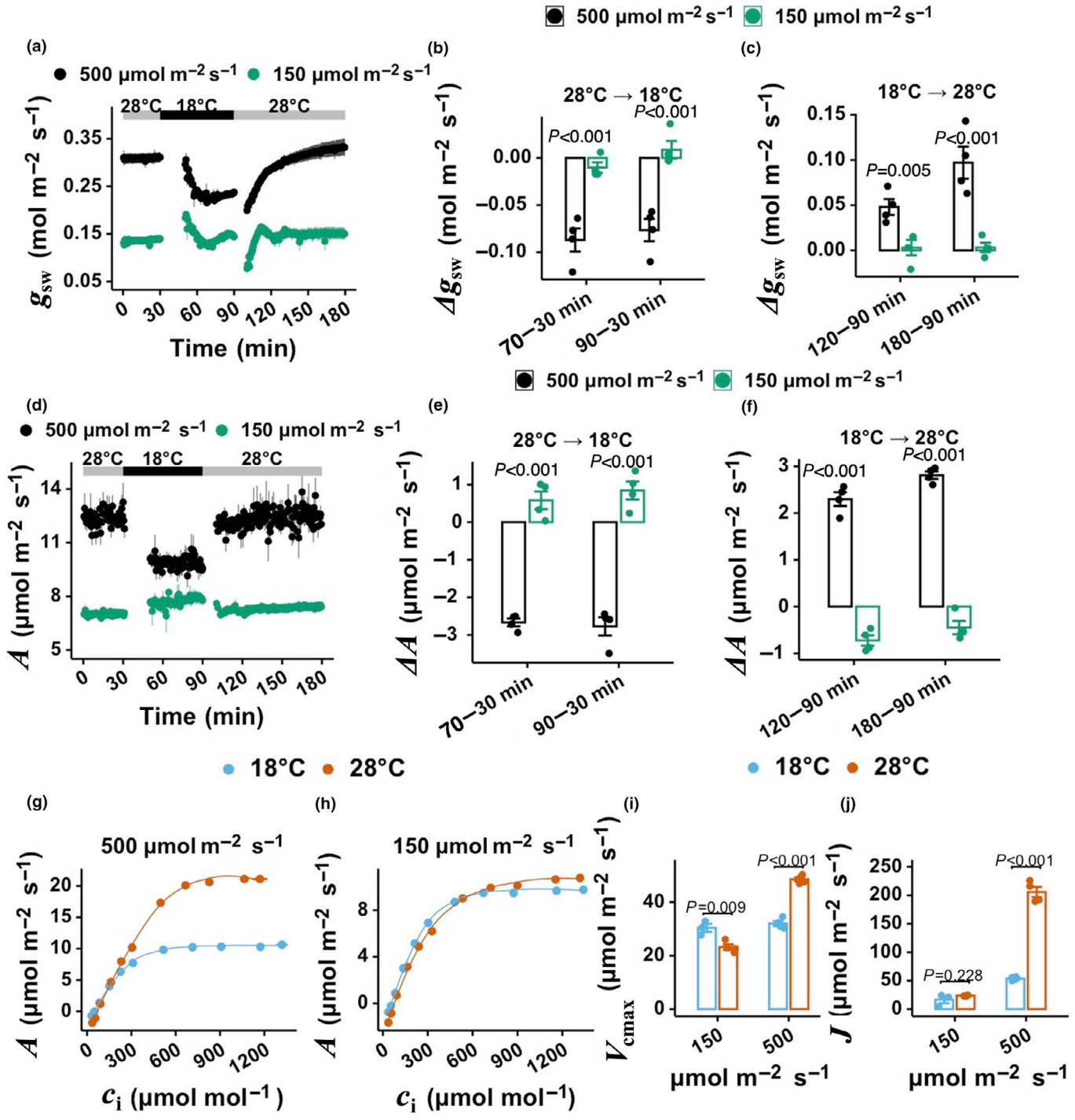

Fig. 6 Low light negates the stomatal and photosynthetic responses to temperature changes. (a) Time-resolved changes in stomatal conductance (g_{sw}) in (a) and CO_2 assimilation (A) in (d) in response to temperature in Col-0 wild-type (WT) leaves under 150 µmol m^{-2} s^{-1} ($n = 4$) and 500 µmol m^{-2} s^{-1} ($n = 4$). Measurements were performed under two light conditions: 450 µmol m^{-2} s^{-1} of red light combined with 50 µmol m^{-2} s^{-1} of blue light and 135 µmol m^{-2} s^{-1} of red light combined with 15 µmol m^{-2} s^{-1} of blue light, a CO_2 concentration of 400 µmol mol^{-1}, and 1.2 kPa of leaf-to-air vapor pressure difference. (b, c, e, f) Changes in stomatal conductance (Δg_{sw}) and CO_2 assimilation (ΔA) in response to temperature decreases in (b, e) and temperature increases in (c, f) were determined as described in the Materials and Methods section. (g, h) Photosynthetic A–c_i response curves of Col-0 WT at 150 µmol m^{-2} s^{-1} ($n = 4$) in (g) and 500 µmol m^{-2} s^{-1} ($n = 4$) in (h). (i, j) Derived parameters from the A–c_i response curve, including (i) maximum carboxylation efficiency ($V_{c_{max}}$) and (j) electron transport rate (J). Note that the same Col-0 WT control data measured at high light of 500 µmol m^{-2} s^{-1} are shown in Fig. 4(a–c) as other mutants were grown in parallel and measured in the same set of experiments. Data represent mean ± SE. Statistical analyses were done using one-way ANOVA with pairwise Tukey's HSD *post hoc* test between the light conditions (Supporting Information Fig. (S13(a–d)). The P-values presented above bar graphs are the same as in Fig. S13(a–d). The direct comparison of light experiments was measured in another set of independent experiments as shown in Fig. S8.

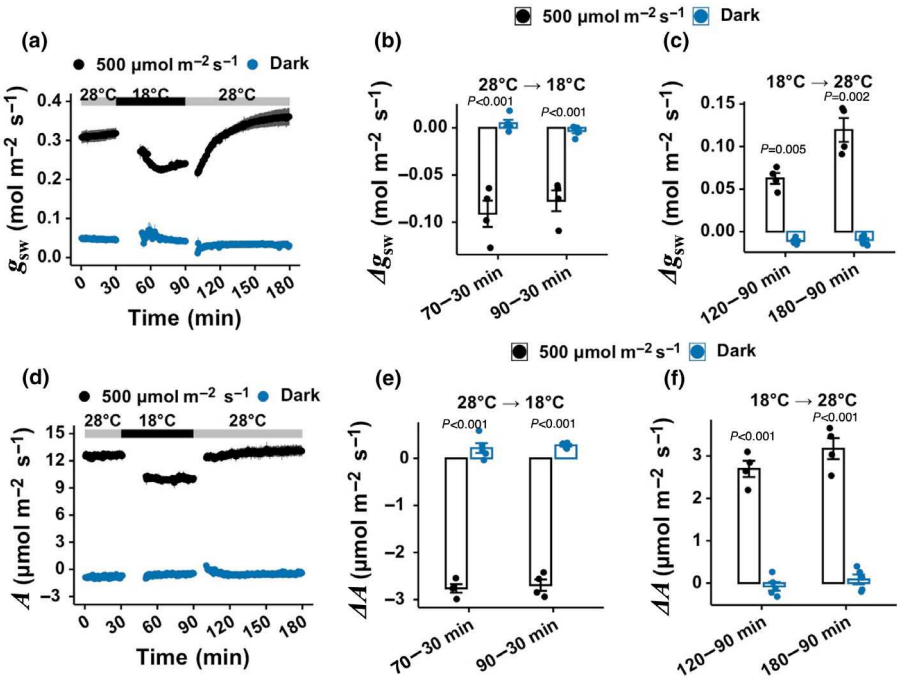

Fig. 7 Darkness disrupts the stomatal responses to temperature changes. (a, d) Time-resolved changes in stomatal conductance (g_{sw}) in (a) and CO_2 assimilation (A) in (d) in response to temperature shifts in Col-0 wild-type (WT) under 500 µmol m^{-2} s^{-1} ($n = 4$) and darkness ($n = 5$). Measurements were performed under two light conditions: 450 µmol m^{-2} s^{-1} of red light combined with 50 µmol m^{-2} s^{-1} of blue light, and darkness (0 µmol m^{-2} s^{-1}), a CO_2 concentration of 400 µmol mol^{-1}, and *c*. 1.2 kPa of leaf-to-air vapor pressure difference. (b, c, e, f) Changes in stomatal conductance (Δg_{sw}) and CO_2 assimilation (ΔA) in response to temperature decreases in (b, e) and temperature increases in (c, f) were determined as described in the Materials and Methods section. Note that the same Col-0 WT control data measured at high light of 500 µmol m^{-2} s^{-1} are shown in Fig. 4(d–f), Supporting Information S2(d–f), S4(a–c), as other mutants were grown in parallel and measured in the same set of experiments. Data represent mean ± SE. Statistical analyses were done using one-way ANOVA with pairwise Tukey's HSD *post hoc* test between the light conditions (see also Figs S18, S19). The *P*-values presented above bar graphs are the same as in Fig. S14(a–d). Light experiments were measured in another set of independent experiments as shown in Supporting Information Fig. S9.

In the dark, temperature increases did not increase CO_2 assimilation rates (Figs 7d–f, S9d–f).

Based on the above findings, we further investigated temperature shift-induced changes in calculated intercellular leaf CO_2 (c_i) concentrations (Figs 8c). These analyses show, as predicted (Farquhar *et al.*, 1978), that c_i transiently shifts in response to temperature changes (Figs 8c), consistent with c_i changes not only initiating the stomatal temperature response but also indicating that additional mechanisms are required for maintaining steady-state temperature-dependent stomatal conductance shifts (see Discussion section).

Discussion

Temperature elevation is known to cause stomatal opening (Darwin, 1898; Raschke, 1970; Rogers *et al.*, 1979). However, the underlying molecular genetic mechanisms remain, to a large degree, unknown. In the present study, we investigated the impact of mutations in known guard cell signal transduction pathways on reversible time-resolved temperature shift-induced stomatal opening and closing. Using a genetics approach, *Arabidopsis* and *Brachypodium* mutants disrupting upstream CO_2 sensing and signaling mechanisms show severely impaired stomatal opening in response to elevated temperatures and stomatal closing in response to low temperatures (Figs 4, 5, S6, S7). Furthermore, a robust warming-induced stomatal opening required exposure to high light and was disrupted under low light fluence rate and darkness (Figs 6a–f, 7a–f, S8a–f, and S9a–f). Examination of CO_2 assimilation rates showed that temperature elevation caused a rapid increase in CO_2 assimilation and an ensuing transient decrease in c_i levels (Fig. 8b, c). Our findings suggest that, upon a temperature increase, low leaf intercellular CO_2 concentrations resulting from a rapid increase in CO_2 assimilation trigger stomatal opening. The molecular pathway for the stomatal response to temperature changes requires the major CO_2 sensing mechanisms in the stomatal CO_2 signaling pathway and may, therefore, be initiated by a rapid reduction in leaf intercellular CO_2 concentration. Moreover, the transient change in leaf internal CO_2 concentration indicates a function for an additional component that maintains stomatal opening upon temperature elevation, as discussed further below.

Stomatal blue light signaling partially contributes to warming-induced stomatal opening

It was recently shown that blue light signaling components contribute to stomatal opening at elevated temperatures of 35°C

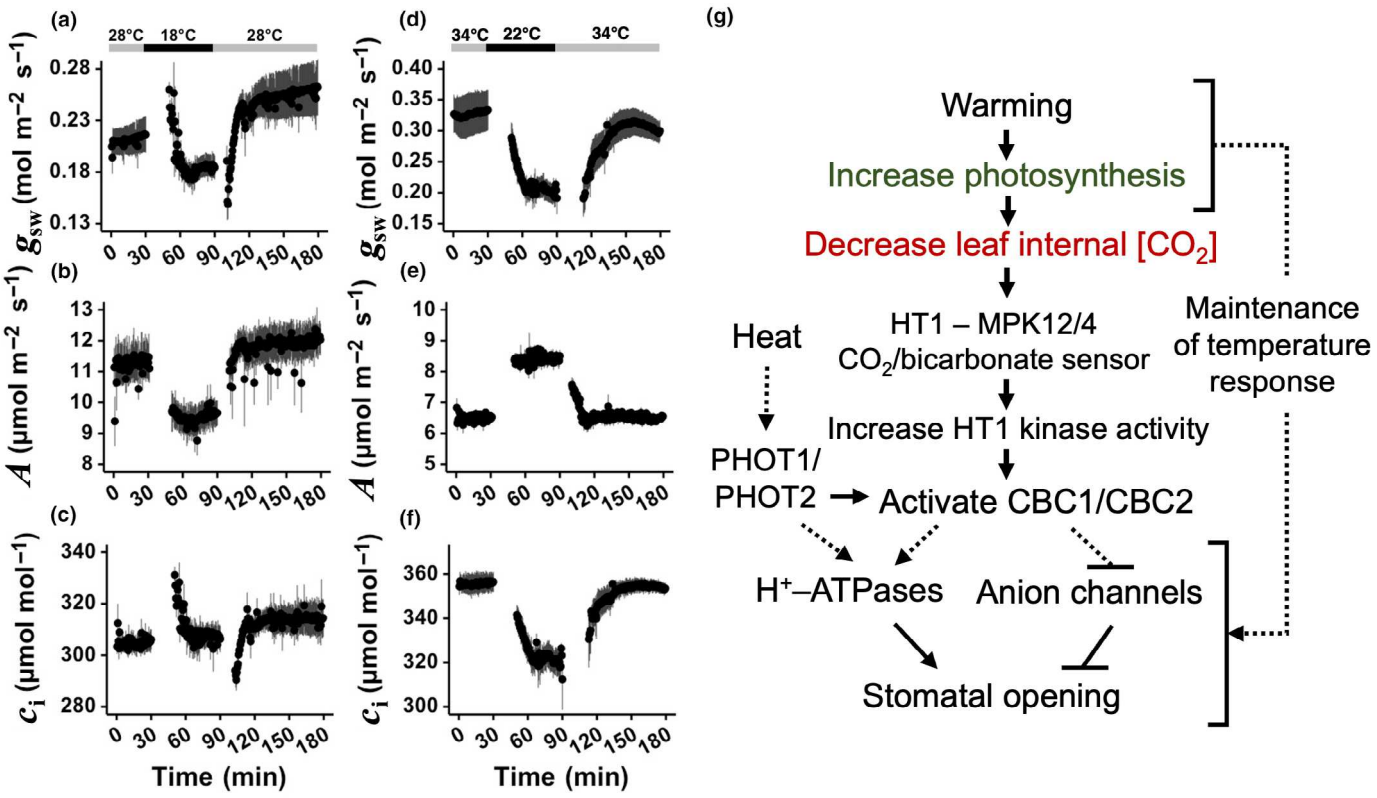

Fig. 8 Distinct effects of 28°C and 34°C temperature shifts on intercellular leaf CO_2 concentrations and model for present findings of genetic and physiological signal transduction mechanisms that strongly regulate stomatal opening to temperature elevation and stomatal closure to temperature reduction. (a–f) Time-resolved measurement of (a, d) stomatal conductance (g_{sw}), (b, e) CO_2 assimilation rates, and (c, f) intercellular CO_2 concentrations in response to indicated leaf temperature (T_{leaf}) shifts in Col-0 wild-type leaves ($n = 4$). (d, f) Time-resolved measurements at higher temperatures from 22 to 34°C (see the Materials and Methods section). (g) The presented data provide consistent evidence that the guard cell warming temperature response is triggered via the early CO_2 sensing and signal transduction pathway with a contribution that depends on PHOT1/PHOT2 (see Results and Discussion sections). Warming temperatures enhance photosynthesis in leaves, thus reducing intercellular CO_2 and initiating stomatal opening via the CO_2/bicarbonate MITOGEN-ACTIVATED PROTEIN KINASE 12 and 4 (MPK12/4)–HIGH TEMPERATURE 1 (HT1) sensor. A further component is required and an energy charge component (Farquhar & Wong, 1984; Buckley *et al*., 2003) is discussed that maintains stomatal opening after a restored level of leaf internal CO_2 concentrations (See Discussion section). At higher temperatures, a decoupling of stomatal opening from photosynthesis occurs (Heat: lower left in g). Recent research has shown a requirement of PHOT1/PHOT2 for the stomatal response to heat stress (Kostaki *et al*., 2020). For (a–c), measurements were performed under 450 µmol m^{-2} s^{-1} of red light combined with 50 µmol m^{-2} s^{-1} of blue light, a CO_2 concentration of 400 µmol mol^{-1}, and a 1.2 kPa leaf-to-air vapor pressure difference. For (d–f), measurements were conducted under the same relative light spectra and CO_2 concentration, except a total light fluence rate of 150 µmol m^{-2} s^{-1} and 1.5 kPa of vapor pressure difference were imposed. Records of stomatal conductance are not shown immediately during the temperature transition (See the Results and Materials and Methods sections). Note that the same data in Fig. 8(a) are shown in Fig. 5(a,g). Data represent mean ± SE. For (d–f), another set of independent experiments shown in Fig. S10 resulted in similar findings.

(Kostaki *et al*., 2020). Our study correlates with this model, based on evidence that *phot1-5/phot2-1* double-mutant leaves show reduced stomatal opening in response to temperature increases to 28°C (Figs 2a–c, S3a–c). Upon blue light exposure, PHOT1 phosphorylates itself and activates the downstream BLUS1 kinase, leading to increased H^+-ATPase activity, resulting in guard cell plasma membrane hyperpolarization and stomatal opening (Takemiya *et al*., 2013). Plasma membrane H^+-ATPases act downstream of PHOT1/PHOT2 and BLUS1 (Kinoshita *et al*., 2001; Takemiya *et al*., 2013). Blue light-induced activation of H^+-ATPase causes guard cell membrane hyperpolarization and subsequent activation of inward-rectifying potassium channels (Assmann *et al*., 1985; Shimazaki *et al*., 1986; Schroeder *et al*., 1987). *ARABIDOPSIS* H^+*-ATPASE 1/2* (*AHA1/AHA2*) are highly expressed in guard cells. However, the *aha1/aha2* double mutant is embryonic lethal (Haruta *et al*., 2010; Kostaki *et al*., 2020). Therefore, the likely role of plasma membrane H^+-ATPases was not investigated in the present study. Temperature shift-induced changes in stomatal conductance were robust in *blus1-3* mutant leaves, with an apparent only slightly reduced stomatal opening response at some time points, which was not consistent in two independent sets of experiments (Figs 2d–f, S3d–f). Note that the different temperature ranges analyzed in the present study (18 to 28°C) and by Kostaki *et al*. (2020; 22 to 35°C) may provide a basis for this difference, as discussed further below.

Interestingly, high temperature-induced stomatal opening is severely impaired in *cbc1/cbc2* double-mutant leaves (Figs 5g–i, S7d–f). CBC1 and CBC2 have been shown to function as blue light and CO_2 signaling components that are required for

blue light inhibition of S-type anion channels (Hiyama *et al.*, 2017). Blue light-induced inhibition of S-type anion channels is impaired in the *phot1-5/phot2-1* double mutant (Marten *et al.*, 2007) and in the *cbc1/cbc2* double mutant (Hiyama *et al.*, 2017). Note that blue light and CO_2 signaling protein kinases phosphorylate CBC1 at different sites and regulate CBC1 via different mechanisms (Hiyama *et al.*, 2017; Takahashi *et al.*, 2022). The impaired stomatal opening in response to temperature elevation of intact leaves (Figs 5g–i, S7d–f) would be consistent with the reduced increase in stomatal aperture at high temperature- in epidermal fragments of the *phot1-5/phot2-1* double mutant (Kostaki *et al.*, 2020). Our findings may be linked to an increase in S-type anion channel activity in the *phot1-5/phot2-1* double mutant due to the lack of phototropin-dependent inhibition (Kinoshita *et al.*, 2001; Marten *et al.*, 2007).

SnRK2.6/OST1 kinase affects stomatal responses

Mutant leaves disrupting the OST1/SnRK2.6 kinase showed impaired stomatal closing in response to temperature decreases in two sets of independent experiments (Fig. S2a–f). The OST1/SnRK2.6 kinase is central to stomatal regulation, affecting many stomatal signaling pathways. The *ost1-3* mutant is insensitive to exogenous ABA and shows impaired stomatal closure in response to high ozone, CO_2, and VPD (Mustilli *et al.*, 2002; Hsu *et al.*, 2018, 2021; Merilo *et al.*, 2018). Interestingly, *nced3-2/nced5-2* double-mutant plants that are impaired in ABA biosynthesis show intact stomatal closing in response to temperature reduction and robust stomatal opening when temperature is increased (Fig. S4a–c). This indicates that temperature reduction-induced stomatal closure may not be linked to a rapid NCED-dependent increase in ABA biosynthesis. An average slightly stronger decrease in stomatal conductance in response to temperature decreases of *nced3-2/nced5-2* double-mutant leaves (Fig. S4b; $P = 0.063$ from 30 min at 28°C to 90 min at 18°C; $n = 4$ plants per genotype) also contrasts with the reduced ABA-induced stomatal closing in ABA-deficient mutants, and may therefore be the result of the larger steady-state stomatal conductance of this mutant (Chater *et al.*, 2015; Hsu *et al.*, 2018). Future studies of ABA receptor mutants could provide additional insights into the role of ABA signaling on guard cell temperature signaling.

Stomatal opening at warm temperatures is mediated by stomatal CO_2/bicarbonate signal transduction

Mutants in the stomatal CO_2 sensor subunit, *ht1-2* and *ht1-A109V* (Takahashi *et al.*, 2022), show severely impaired stomatal responses to temperature changes (Figs 4a–f, S6a–f). In addition, silencing alleles in *mpk12/mpk4-gc*, and *Brachypodium Bdmpk5* knockout plants and *cbc1/cbc2* double mutants showed impaired temperature responses (Figs 5a–i, S7a–f). These data demonstrate that guard cell CO_2/bicarbonate signaling mechanisms play a central role in driving the stomatal warm temperature response. A recent study showed that BdMPK5 protein was able to reconstitute high CO_2/bicarbonate-induced inhibition of HT1 kinase activity, suggesting that BdMPK5 is a component of the CO_2 sensor in *Brachypodium* (Lopez *et al.*, 2024). The strongly impaired stomatal warming responses of MAP kinase mutant plants in both *Arabidopsis* and *Brachypodium* (Fig. 5) indicate a conserved genetic requirement of CO_2/bicarbonate sensing components (Takahashi *et al.*, 2022; Lopez *et al.*, 2024) for the stomatal warming response across C3 dicot and monocot species.

We further show that cooling-induced stomatal closure and warming-induced stomatal opening depend on a high light fluence rate. When the temperature increased from 18°C to 28°C under high light (500 µmol m^{-2} s^{-1}), an increase in stomatal conductance coincided with an increased CO_2 assimilation rate (Figs 6a–f, S8a–f). Furthermore, these high light conditions caused a higher $V_{c_{max}}$ and J at 28°C (Fig. 6i,j). These findings are consistent with a warming-induced increase in the CO_2 assimilation rate (Raschke, 1970; Farquhar & von Caemmerer, 1982). At a low fluence rate of 150 µmol m^{-2} s^{-1}, we found that CO_2 assimilation decreased slightly in response to temperature elevation (Fig. 6d–f), likely due to limited RuBP regeneration under light-limiting photosynthesis (Mott *et al.*, 1984). This observation may be linked to a temperature elevation-induced increase in dark respiration (Mohammed & Tarpley, 2009). Similarly, a recent study showed that the nocturnal stomatal conductance in spring wheat (*Triticum aestivum*) decreased between 9% and 33% under high night temperatures rather than increasing (McAusland *et al.*, 2021).

A model linking stomatal temperature sensing and signaling response to leaf intercellular CO_2 concentrations

Having identified essential genetic components of the signaling pathway and found no or limited effects of some of the examined other potential contributors, we can build a basic molecular genetic framework for stomatal sensing and response to temperature warming. The involvement of several key protein kinases that are directly associated with stomatal CO_2 sensing and early signal transduction (Figs 4, 5, S6, S7) and the dependence of stomatal temperature sensitivity on light fluence rate (Figs 6, 7, S8, S9) points to a role of leaf intercellular CO_2 concentration as a trigger of the stomatal temperature response to warm temperatures. Our finding aligns with the study by Ando *et al.* (2022) that elevated CO_2 levels cause dephosphorylation of the penultimate threonine residue of plasma membrane H^+-ATPases in guard cells, which contributes to stomatal closing.

It is well established that, as daily environmental variables affecting photosynthesis and transpiration change, stomata tend to respond in a way that maintains the ratio of atmospheric to leaf internal CO_2 concentration relatively constant (Wong *et al.*, 1979), although the mean value of this ratio tends to shift slightly with adaptation to more humid or more arid environments (Franks *et al.*, 2017). With atmospheric CO_2 concentration remaining relatively constant in the short term, environmental fluctuations that affect intercellular CO_2 concentrations will be counteracted by stomatal movements that tend to return intercellular CO_2 levels relatively close to prestimulus levels (Fig. 8c). The basic mechanism for this involves the operation of two negative feedback loops that

control the influence of stomatal conductance and CO_2 assimilation rate on the intercellular CO_2 concentration (Farquhar *et al.*, 1978). We found *c.* 30 μmol mol^{-1} reduction in the intercellular CO_2 level at 10 min after temperature increases from 18°C to 28°C (Fig. 8c). An increase in stomatal conductance was observed despite the restoration of leaf internal CO_2 levels by the first 30 min of temperature elevation (Fig. 8a–c). Our results suggest that the stomatal response to temperature may be linked initially to the control of intercellular CO_2 concentration through the action of these feedback loops, the rationale being that an increase in leaf temperature directly stimulates photosynthetic biochemistry, initially lowering intercellular CO_2 level and initiating stomatal conductance increases to restore intercellular CO_2 (Fig. 8g).

A question remains, however, as to why stomatal conductance increases are not transient or oscillating as a function of the negative feedback loop upon warm temperature exposure, given that leaf internal CO_2 changes are transient (Fig. 8c). In addition to the role of the low internal CO_2 response, our findings implicate an additional important factor(s) involved in maintaining stomatal opening in response to elevated temperature. For example, increased photochemical activity in leaf mesophyll and guard cells could be linked to an increased metabolic energy supply that may be used for stomatal opening, as hypothesized in previous studies (Farquhar & Wong, 1984; Buckley *et al.*, 2003). Increased energy production from light reactions of mesophyll and guard cells may be one of the factors driving stomatal opening in response to elevated temperature. Recently, it has been reported that energy transport from the mesophyll is directly linked to light-induced stomatal opening (Lim *et al.*, 2022). Lim *et al.* (2022) found that guard cell ATP transporters facilitating cytosolic ATP import, likely from neighboring mesophyll cells, enhance light-induced stomatal opening. In response to warm temperatures at high light, increased ATP levels, for example, may energize stomatal opening but may not necessarily be the signal that induces stomatal opening, in line with findings of the strong requirement for CO_2 sensing and signaling components (Figs 4, 5, 8g, S6, S7).

As noted earlier, the temperature range in the present study of 18°C to 28°C differs from recent studies at 35°C (Kostaki *et al.*, 2020) and at 37°C (Korte *et al.*, 2023). A temperature of 28°C is known to cause stress responses in *Arabidopsis thaliana* (Ludwig-Müller *et al.*, 2000; Li *et al.*, 2018; Kerbler & Wigge, 2023). We attempted approaches to measure further increased temperatures in the leaves of intact plants while maintaining a stable VPD_{leaf}. We were able to establish an approach that enabled stable VPD_{leaf} upon transition to 34°C (See Materials and Methods section). Using this approach, we observed the expected heat-induced stomatal opening upon exposure to 34°C (Figs 8d, S10a). Simultaneously measured CO_2 assimilation rates at 34°C showed that stomata continued to open, even though CO_2 assimilation rates were reduced, resulting in an increased leaf internal CO_2 concentration (Figs 8e,f, S10b,c). Our findings align with the reported uncoupling of stomatal conductance and photosynthesis upon heat exposure (Raschke, 1970; Urban *et al.*, 2017; Marchin *et al.*, 2023; Diao *et al.*, 2024). Thus, at high temperatures, where CO_2 assimilation rates decline, additional nonphotosynthesis-dependent mechanisms, including PHOT1 and PHOT2 (Kostaki *et al.*, 2020), may play a key role in promoting leaf evaporative cooling in response to heat stress (Figs 8d–f, S10a–c).

We performed the present noninvasive gas exchange assays with intact leaves attached to intact plants where the physiological context of leaves remains preserved. This has allowed us to resolve the influence of CO_2 assimilation and leaf internal CO_2 concentration on the rapid stomatal response to temperature changes. We determined stomatal temperature responses by comparing absolute changes in stomatal conductance in response to temperature shifts. Since we performed gas exchange measurements of fully expanded leaves over a short time period, stomatal development has already occurred and is not affected. Arguably, such stomatal conductance responses could be linked to differences in stomatal density. Previous studies have analyzed the stomatal density of several mutants presented in this study. The stomatal density of *ht1-2* mutant leaves (Hashimoto *et al.*, 2006) *ht1-A109V* mutant leaves (Hõrak *et al.*, 2016) and *ost1-3* mutant leaves (Merilo *et al.*, 2018) are similar to Col-0 WT. On the other hand, in *mpk12/4-gc* mutant leaves, a stomatal index is slightly lower than WT despite larger stomatal conductance (Tõldsepp *et al.*, 2018). Impaired stomatal conductance responses to temperature shifts in strong mutants in the present study demonstrate that impaired stomatal temperature responses occur despite similar or slightly different and opposite stomatal densities from Col-0 WT controls.

Conclusions

We report an improved gas exchange measurement approach to investigate time-resolved stomatal conductance changes in response to temperature shifts in intact leaves attached to intact plants while stabilizing vapor pressure differences between leaves and air. We investigated mutants disrupting stomatal signaling to blue light, CO_2, ABA synthesis, and putative temperature sensor proteins. Our findings show that the temperature sensing phyB and ELF3 are not primary temperature sensors in regulating stomatal conductance in response to warm temperatures. Stomatal opening in response to warm temperature is partially impaired in blue light sensor *phot1-5/phot2-1* double-mutant leaves, consistent with recent findings (Kostaki *et al.*, 2020). Interestingly, mutants disrupting downstream BLUS1 kinase show robust stomatal conductance responses to the imposed warming temperature shifts. Phototropins can activate another downstream blue light signaling branch that down-regulates anion channel activity (Hiyama *et al.*, 2017), consistent with the present impaired stomatal temperature response of *slac1-4/slah3-1/almt12-2* triple-mutant leaves. Notably, we find that warming-induced stomatal opening and cooling-induced stomatal closing are strongly impaired in loss-of-function mutants in the CO_2 sensor HT1, MPK12/MPK4, and early CO_2 signaling CBC1/CBC2 components, as well as in CRISPR deletion plants in the monocot grass *Brachypodium distachyon* ortholog (Lopez *et al.*, 2024) of *AtMPK12/AtMPK4*.

We show that elevation to a warm temperature of 28°C rapidly increases CO_2 assimilation rates and, therefore, depletes internal leaf CO_2 concentrations, which in turn signals stomatal opening in intact leaves. Our findings support a model in which CO_2 sensing and signal transduction mechanisms play a key role in triggering warming-induced stomatal opening via responding to reduced c_i levels (Fig. 8g). Furthermore, warming-induced stomatal opening is abolished in darkness, which is consistent with this model. An additional mechanism, for instance, the potential energy supply to guard cells (Farquhar & Wong, 1984; Buckley *et al.*, 2003), is further proposed to aid in maintaining increased stomatal conductance when temperature increases (Fig. 8g). Further research will be required to investigate this second proposed energy supply model for stomatal temperature responses.

The present study further provides compelling evidence that distinct pathways contribute to a stomatal opening at warm (28°C) and high temperatures (34°C), with the higher temperatures decoupling stomatal conductance and photosynthetic CO_2 assimilation (Figs 8d–f,g, S10a–c) (Urban *et al.*, 2017; Marchin *et al.*, 2023; Diao *et al.*, 2024). This latter higher temperature response will require further genetic dissection, in addition to recent relevant studies (Kostaki *et al.*, 2020; Korte *et al.*, 2023). The present findings could be important for ecological and agricultural studies of responses of plants to elevated temperatures during daytime and during nighttime in light of global warming.

Acknowledgements

We thank Drs Diego Marquez, Suan Chin Wong, and Graham Farquhar for their critical discussions and valuable suggestions on improving gas exchange techniques, and Dr Karnelia Paul for helping with plant cultivation. We thank Drs Toshinori Kinoshita (*phot1/phot2* double mutant and *blus1-3* mutant), and Hannes Kollist (*slac1-4/slah3-1/almt12-2* triple mutant) for providing mutant seeds. This research was supported by grants from the Human Frontier Science Program RGP0016/2020 (to PJF and JIS) and the National Science Foundation MCB 1900567 and MCB 2401310 (to JIS). NP was supported by a Thai Royal Government Fellowship in Science and Technology.

Competing interests

None declared.

Author contributions

NP and JIS planned and designed experiments. PH conducted pilot experiments and generated preliminary data. PJF and JIS planned the research and provided advice on techniques. NP developed and standardized the gas exchange techniques, carried out the experiments, analyzed all the data shown in this manuscript, and further developed a working model with JIS. BNKL isolated *Bdmpk5* CRISPR plants. NP and JIS wrote the manuscript with feedback from all authors.

ORCID

Peter J. Franks https://orcid.org/0000-0002-4810-658X
Po-Kai Hsu https://orcid.org/0000-0001-7265-7077
Bryn N. K. Lopez https://orcid.org/0009-0009-3728-8216
Nattiwong Pankasem https://orcid.org/0000-0002-3200-9056
Julian I. Schroeder https://orcid.org/0000-0002-3283-5972

Data availability

Raw data presented in this study can be found on the GitHub repository (https://github.com/nattiwongpan/Pankasem-et-al.-2024-New-Phytol).

References

Ando E, Kollist H, Fukatsu K, Kinoshita T, Terashima I. 2022. Elevated CO_2 induces rapid dephosphorylation of plasma membrane H^+-ATPase in guard cells. *New Phytologist* **236**: 2061–2074.

Assmann SM, Simoncini L, Schroeder JI. 1985. Blue light activates electrogenic ion pumping in guard cell protoplasts of *Vicia faba*. *Nature* **318**: 285–287.

Bates GW, Rosenthal DM, Sun J, Chattopadhyay M, Peffer E, Yang J, Ort DR, Jones AM. 2012. A comparative study of the *Arabidopsis thaliana* guard-cell transcriptome and its modulation by sucrose. *PLoS ONE* **7**: e49641.

Brandt B, Brodsky DE, Xue S, Negi J, Iba K, Kangasjärvi J, Ghassemian M, Stephan AB, Hu H, Schroeder JI. 2012. Reconstitution of abscisic acid activation of SLAC1 anion channel by CPK6 and OST1 kinases and branched ABI1 PP2C phosphatase action. *Proceedings of the National Academy of Sciences, USA* **109**: 10593–10598.

Buckley TN, Mott KA, Farquhar GD. 2003. A hydromechanical and biochemical model of stomatal conductance. *Plant, Cell & Environment* **26**: 1767–1785.

Chater C, Peng K, Movahedi M, Dunn JA, Walker HJ, Liang YK, McLachlan DH, Casson S, Isner JC, Wilson I *et al.* 2015. Elevated CO_2-induced responses in stomata require ABA and ABA signaling. *Current Biology* **25**: 2709–2716.

Clark JW, Harris BJ, Hetherington AJ, Hurtado-Castano N, Brench RA, Casson S, Williams TA, Gray JE, Hetherington AM. 2022. The origin and evolution of stomata. *Current Biology* **32**: R539–R553.

Covington MF, Panda S, Liu XL, Strayer CA, Wagner DR, Kay SA. 2001. ELF3 modulates resetting of the circadian clock in Arabidopsis. *Plant Cell* **13**: 1305–1315.

Darwin F. 1898. IX. Observations on stomata. *Philosophical Transactions of the Royal Society of London. Series B: Biological Sciences* **190**: 531–621.

Diao H, Cernusak LA, Saurer M, Gessler A, Siegwolf RTW, Lehmann MM. 2024. Uncoupling of stomatal conductance and photosynthesis at high temperatures: mechanistic insights from online stable isotope techniques. *New Phytologist* **241**: 2366–2378.

Duursma RA. 2015. Plantecophys – an R package for analysing and modelling leaf gas exchange data. *PLoS ONE* **10**: e0143346.

Farquhar G, Wong S. 1984. An empirical model of stomatal conductance. *Functional Plant Biology* **11**: 191–210.

Farquhar GD, Dubbe DR, Raschke K. 1978. Gain of the feedback loop involving carbon dioxide and stomata: theory and measurement. *Plant Physiology* **62**: 406–412.

Farquhar GD, von Caemmerer S. 1982. Modelling of photosynthetic response to environmental conditions. *Physiological Plant Ecology* **2**: 549–587.

Farquhar GD, von Caemmerer S, Berry JA. 1980. A biochemical model of photosynthetic CO_2 assimilation in leaves of C_3 species. *Planta* **149**: 78–90.

Flütsch S, Nigro A, Conci F, Fajkus J, Thalmann M, Trtílek M, Panzarová K, Santelia D. 2020. Glucose uptake to guard cells via STP transporters provides

carbon sources for stomatal opening and plant growth. *EMBO Reports* **21**: e49719.

Franks PJ, Berry JA, Lombardozzi DL, Bonan GB. 2017. Stomatal function across temporal and spatial scales: deep-time trends, land-atmosphere coupling and global models. *Plant Physiology* **174**: 583–602.

Frey A, Effroy D, Lefebvre V, Seo M, Perreau F, Berger A, Sechet J, To A, North HM, Marion-Poll A. 2012. Epoxycarotenoid cleavage by NCED5 fine-tunes ABA accumulation and affects seed dormancy and drought tolerance with other NCED family members. *The Plant Journal* **70**: 501–512.

Geiger D, Scherzer S, Mumm P, Stange A, Marten I, Bauer H, Ache P, Matschi S, Liese A, Al-Rasheid KAS *et al.* 2009. Activity of guard cell anion channel SLAC1 is controlled by drought-stress signaling kinase-phosphatase pair. *Proceedings of the National Academy of Sciences, USA* **106**: 21425–21430.

Grossiord C, Buckley TN, Cernusak LA, Novick KA, Poulter B, Siegwolf RTW, Sperry JS, McDowell NG. 2020. Plant responses to rising vapor pressure deficit. *New Phytologist* **226**: 1550–1566.

Haruta M, Burch HL, Nelson RB, Barrett-Wilt G, Kline KG, Mohsin SB, Young JC, Otegui MS, Sussman MR. 2010. Molecular characterization of mutant Arabidopsis plants with reduced plasma membrane proton pump activity. *Journal of Biological Chemistry* **285**: 17918–17929.

Hashimoto M, Negi J, Young J, Israelsson M, Schroeder JI, Iba K. 2006. Arabidopsis HT1 kinase controls stomatal movements in response to CO_2. *Nature Cell Biology* **8**: 391–397.

Hiyama A, Takemiya A, Munemasa S, Okuma E, Sugiyama N, Tada Y, Murata Y, Shimazaki KI. 2017. Blue light and CO_2 signals converge to regulate light-induced stomatal opening. *Nature Communications* **8**: 1284.

Hõrak H, Sierla M, Tõldsepp K, Wang C, Wang Y-S, Nuhkat M, Valk E, Pechter P, Merilo E, Salojärvi J *et al.* 2016. A dominant mutation in the HT1 kinase uncovers roles of MAP kinases and GHR1 in CO_2-induced stomatal closure. *Plant Cell* **28**: 2493–2509.

Hsu PK, Takahashi Y, Merilo E, Costa A, Zhang L, Kernig K, Lee KH, Schroeder JI. 2021. Raf-like kinases and receptor-like (pseudo)kinase GHR1 are required for stomatal vapor pressure difference response. *Proceedings of the National Academy of Sciences, USA* **118**: 2107280118.

Hsu PK, Takahashi Y, Munemasa S, Merilo E, Laanemets K, Waadt R, Pater D, Kollist H, Schroeder JI. 2018. Abscisic acid-independent stomatal CO_2 signal transduction pathway and convergence of CO_2 and ABA signaling downstream of OST1 kinase. *Proceedings of the National Academy of Sciences, USA* **115**: E9971–E9980.

Ilan N, Moran N, Schwartz A. 1995. The role of potassium channels in the temperature control of stomatal aperture. *Plant Physiology* **108**: 1161–1170.

IPCC. 2023. *Climate change 2023: impacts, adaptation and vulnerability.* Cambridge, UK and New York, NY USA: Cambridge University Press.

Iuchi S, Kobayashi M, Taji T, Naramoto M, Seki M, Kato T, Tabata S, Kakubari Y, Yamaguchi-Shinozaki K, Shinozaki K. 2001. Regulation of drought tolerance by gene manipulation of 9-*cis*-epoxycarotenoid dioxygenase, a key enzyme in abscisic acid biosynthesis in Arabidopsis. *The Plant Journal* **27**: 325–333.

Jalakas P, Nuhkat M, Vahisalu T, Merilo E, Brosché M, Kollist H. 2021. Combined action of guard cell plasma membrane rapid- and slow-type anion channels in stomatal regulation. *Plant Physiology* **187**: 2126–2133.

Jung JH, Barbosa AD, Hutin S, Kumita JR, Gao M, Derwort D, Silva CS, Lai X, Pierre E, Geng F *et al.* 2020. A prion-like domain in ELF3 functions as a thermosensor in Arabidopsis. *Nature* **585**: 256–260.

Keller BU, Hedrich R, Raschke K. 1989. Voltage-dependent anion channels in the plasma membrane of guard cells. *Nature* **341**: 450–453.

Kerbler SM, Wigge PA. 2023. Temperature sensing in plants. *Annual Review of Plant Biology* **74**: 341–366.

Kinoshita T, Doi M, Suetsugu N, Kagawa T, Wada M, Shimazaki K. 2001. phot1 and phot2 mediate blue light regulation of stomatal opening. *Nature* **414**: 656–660.

Korte P, Unzner A, Damm T, Berger S, Krischke M, Mueller MJ. 2023. High triacylglycerol turnover is required for efficient opening of stomata during heat stress in Arabidopsis. *The Plant Journal* **115**: 81–96.

Kostaki KI, Coupel-Ledru A, Bonnell VC, Gustavsson M, Sun P, McLaughlin FJ, Fraser DP, McLachlan DH, Hetherington AM, Dodd AN *et al.* 2020. Guard cells integrate light and temperature signals to control stomatal aperture. *Plant Physiology* **182**: 1404–1419.

Lawson T, Lefebvre S, Baker NR, Morison JIL, Raines CA. 2008. Reductions in mesophyll and guard cell photosynthesis impact on the control of stomatal responses to light and CO_2. *Journal of Experimental Botany* **59**: 3609–3619.

Lee SC, Lan W, Buchanan BB, Luan S. 2009. A protein kinase-phosphatase pair interacts with an ion channel to regulate ABA signaling in plant guard cells. *Proceedings of the National Academy of Sciences, USA* **106**: 21419–21424.

Legris M, Klose C, Burgie ES, Rojas CC, Neme M, Hiltbrunner A, Wigge PA, Schäfer E, Vierstra RD, Casal JJ. 2016. Phytochrome B integrates light and temperature signals in Arabidopsis. *Science* **354**: 897–900.

Li B, Gao K, Ren H, Tang W. 2018. Molecular mechanisms governing plant responses to high temperatures. *Journal of Integrative Plant Biology* **60**: 757–779.

Lim SL, Flütsch S, Liu J, Distefano L, Santelia D, Lim BL. 2022. Arabidopsis guard cell chloroplasts import cytosolic ATP for starch turnover and stomatal opening. *Nature Communications* **13**: 652.

Lopez BNK, Ceciliato PHO, Takahashi Y, Rangel FJ, Salem EA, Kernig K, Chow K, Zhang L, Sidhom MA, Seitz CG *et al.* 2024. CO_2 response screen in grass Brachypodium reveals the key role of a MAP kinase in CO_2-triggered stomatal closure. *Plant Physiology* **20**: kiae262.

Ludwig-Müller J, Krishna P, Forreiter C. 2000. A glucosinolate mutant of arabidopsis is thermosensitive and defective in cytosolic Hsp90 expression after heat stress1. *Plant Physiology* **123**: 949–958.

Ma Y, Szostkiewicz I, Korte A, Moes D, Yang Y, Christmann A, Grill E. 2009. Regulators of PP2C phosphatase activity function as abscisic acid sensors. *Science* **324**: 1064–1068.

Marchin RM, Medlyn BE, Tjoelker MG, Ellsworth DS. 2023. Decoupling between stomatal conductance and photosynthesis occurs under extreme heat in broadleaf tree species regardless of water access. *Global Change Biology* **29**: 6319–6335.

Marten H, Hedrich R, Roelfsema MRG. 2007. Blue light inhibits guard cell plasma membrane anion channels in a phototropin-dependent manner. *The Plant Journal* **50**: 29–39.

Matthews JSA, Vialet-Chabrand S, Lawson T. 2020. Role of blue and red light in stomatal dynamic behaviour. *Journal of Experimental Botany* **71**: 2253–2269.

McAusland L, Smith KE, Williams A, Molero G, Murchie EH. 2021. Nocturnal stomatal conductance in wheat is growth-stage specific and shows genotypic variation. *New Phytologist* **232**: 162–175.

Merilo E, Yarmolinsky D, Jalakas P, Parik H, Tulva I, Rasulov B, Kilk K, Kollist H. 2018. Stomatal VPD response: there is more to the story than ABA. *Plant Physiology* **176**: 851–864.

Meyer S, Mumm P, Imes D, Endler A, Weder B, Al-Rasheid KAS, Geiger D, Marten I, Martinoia E, Hedrich R. 2010. AtALMT12 represents an R-type anion channel required for stomatal movement in Arabidopsis guard cells. *The Plant Journal* **63**: 1054–1062.

Mohammed AR, Tarpley L. 2009. Impact of high nighttime temperature on respiration, membrane stability, antioxidant capacity, and yield of rice plants. *Crop Science* **49**: 313–322.

Mott KA. 1988. Do stomata respond to CO_2 concentrations other than intercellular? *Plant Physiology* **86**: 200–203.

Mott KA, Jensen RG, O'leary JW, Berry JA. 1984. Photosynthesis and ribulose 1,5-bisphosphate concentrations in intact leaves of *Xanthium Strumarium* L. *Plant Physiology* **76**: 968–971.

Mott KA, Sibbernsen ED, Shope JC. 2008. The role of the mesophyll in stomatal responses to light and CO_2. *Plant, Cell & Environment* **31**: 1299–1306.

Mustilli AC, Merlot S, Vavasseur A, Fenzi F, Giraudat J. 2002. Arabidopsis OST1 protein kinase mediates the regulation of stomatal aperture by abscisic acid and acts upstream of reactive oxygen species production. *Plant Cell* **14**: 3089–3099.

Negi J, Matsuda O, Nagasawa T, Oba Y, Takahashi H, Kawai-Yamada M, Uchimiya H, Hashimoto M, Iba K. 2008. CO_2 regulator SLAC1 and its homologues are essential for anion homeostasis in plant cells. *Nature* **452**: 483–486.

Pandey S, Wang RS, Wilson L, Li S, Zhao Z, Gookin TE, Assmann SM, Albert R. 2010. Boolean modeling of transcriptome data reveals novel modes of heterotrimeric G-protein action. *Molecular Systems Biology* **6**: 372.

Pandey S, Zhang W, Assmann SM. 2007. Roles of ion channels and transporters in guard cell signal transduction. *FEBS Letters* **581**: 2325–2336.

Park SY, Fung P, Nishimura N, Jensen DR, Fujii H, Zhao Y, Lumba S, Santiago J, Rodrigues A, Chow TFF *et al.* 2009. Abscisic acid inhibits type 2C

protein phosphatases via the PYR/PYL family of START proteins. *Science* **324**: 1068–1071.

Raschke K. 1970. Temperature dependence of CO_2 assimilation and stomatal aperture in leaf sections of Zea mays. *Planta* **91**: 336–363.

Reed JW, Nagpal P, Poole DS, Furuya M, Chory J. 1993. Mutations in the gene for the red/far-red light receptor phytochrome B alter cell elongation and physiological responses throughout Arabidopsis development. *Plant Cell* **5**: 147–157.

Roelfsema MRG, Hanstein S, Felle HH, Hedrich R. 2002. CO_2 provides an intermediate link in the red light response of guard cells. *The Plant Journal* **32**: 65–75.

Rogers CA, Powell RD, Sharpe PJH. 1979. Relationship of temperature to stomatal aperture and potassium accumulation in guard cells of *Vicia faba*. *Plant Physiology* **63**: 388–391.

Running SW. 1976. Environmental control of leaf water conductance in conifers. *Canadian Journal of Forest Research* **6**: 104–112.

Sakata T, Oshino T, Miura S, Tomabechi M, Tsunaga Y, Higashitani N, Miyazawa Y, Takahashi H, Watanabe M, Higashitani A. 2010. Auxins reverse plant male sterility caused by high temperatures. *Proceedings of the National Academy of Sciences, USA* **107**: 8569–8574.

Schroeder JI, Hagiwara S. 1989. Cytosolic calcium regulates ion channels in the plasma membrane of *Vicia faba* guard cells. *Nature* **338**: 427–430.

Schroeder JI, Raschke K, Neher E. 1987. Voltage dependence of K^+ channels in guard-cell protoplasts. *Proceedings of the National Academy of Sciences, USA* **84**: 4108–4112.

Schroeder JI, Schmidt C, Sheaffer J. 1993. Identification of high-affinity slow anion channel blockers and evidence for stomatal regulation by slow anion channels in guard cells. *Plant Cell* **5**: 1831–1841.

Shimazaki K, Iino M, Zeiger E. 1986. Blue light-dependent proton extrusion by guard-cell protoplasts of *Vicia faba*. *Nature* **319**: 324–326.

Takahashi Y, Bosmans KC, Hsu PK, Paul K, Seitz C, Yeh CY, Wang YS, Yarmolinsky D, Sierla M, Vahisalu T *et al.* 2022. Stomatal CO_2/bicarbonate sensor consists of two interacting protein kinases, Raf-like HT1 and nonkinase-activity activity requiring MPK12/MPK4. *Science Advances* **8**: eabq6161.

Takemiya A, Sugiyama N, Fujimoto H, Tsutsumi T, Yamauchi S, Hiyama A, Tada Y, Christie JM, Shimazaki KI. 2013. Phosphorylation of BLUS1 kinase by phototropins is a primary step in stomatal opening. *Nature Communications* **4**: 1–8.

Tõldsepp K, Zhang J, Takahashi Y, Sindarovska Y, Hõrak H, Ceciliato PHO, Koolmeister K, Wang YS, Vaahtera L, Jakobson L *et al.* 2018. Mitogen-activated protein kinases MPK4 and MPK12 are key components mediating CO_2-induced stomatal movements. *The Plant Journal* **96**: 1018–1035.

Urban J, Ingwers MW, McGuire MA, Teskey RO. 2017. Increase in leaf temperature opens stomata and decouples net photosynthesis from stomatal conductance in *Pinus taeda* and *Populus deltoides* × *nigra*. *Journal of Experimental Botany* **68**: 1757–1767.

Vahisalu T, Kollist H, Wang YF, Nishimura N, Chan WY, Valerio G, Lamminmäki A, Brosché M, Moldau H, Desikan R *et al.* 2008. SLAC1 is required for plant guard cell S-type anion channel function in stomatal signalling. *Nature* **452**: 487–491.

Wong SC, Cowan IR, Farquhar GD. 1979. Stomatal conductance correlates with photosynthetic capacity. *Nature* **282**: 424–426.

Yang Y, Costa A, Leonhardt N, Siegel RS, Schroeder JI. 2008. Isolation of a strong Arabidopsis guard cell promoter and its potential as a research tool. *Plant Methods* **4**: 6.

Yoshida R, Hobo T, Ichimura K, Mizoguchi T, Takahashi F, Aronso J, Ecker JR, Shinozaki K. 2002. ABA-activated SnRK2 protein kinase is required for dehydration stress signaling in Arabidopsis. *Plant and Cell Physiology* **43**: 1473–1483.

Yoshida Y, Sarmiento-Mañús R, Yamori W, Ponce MR, Micol JL, Tsukaya H. 2018. The arabidopsis phyB-9 mutant has a second-site mutation in the VENOSA4 gene that alters chloroplast size, photosynthetic traits, and leaf growth. *Plant Physiology* **178**: 3–6.

Supporting Information

Additional Supporting Information may be found online in the Supporting Information section at the end of the article.

Fig. S1 *slac1-4/slah3-1/almt12-2* triple-mutant leaves impairing S-type and R-type anion channels show impaired stomatal responses to temperature changes.

Fig. S2 *ost1-3* mutant leaves lacking the SnRK2.6 kinase show impaired stomatal responses to temperature changes in two independent sets of experiments.

Fig. S3 Stomatal blue light signaling partially contributes to warming-induced stomatal opening.

Fig. S4 Stomatal response to temperature shifts in the ABA-biosynthesis *nced3-2/nced5-2* double-mutant leaves.

Fig. S5 *phyB-9* mutant and *elf3-1* mutant do not show a dramatic effect on stomatal responses to temperature changes.

Fig. S6 Stomatal responses to temperature shifts are severely impaired in CO_2/bicarbonate sensing *ht1-2* mutant and *ht1-A109V* mutant leaves.

Fig. S7 *mpk12/4-gc* and *cbc1/cbc2* double-mutant leaves show severely impaired stomatal responses to temperature shifts.

Fig. S8 Low light negates the stomatal and photosynthetic responses to temperature changes.

Fig. S9 Darkness disrupts the stomatal responses to temperature changes.

Fig. S10 Uncoupled responses of stomatal conductance and CO_2 assimilation at high temperature.

Fig. S11 Statistical comparison of *cbc1/cbc2* double mutant, *mpk12/4-gc-1* double mutant, and *mpk12/4-gc-2* double mutant with Col-0 wild-type control measured in the same set of experiments.

Fig. S12 Statistical comparison of *phot1-5/phot2-1* double mutant, *ost1-3* mutant, *and slac1-4/slah3-1/almt12-2* triple mutant with Col-0 wild-type control measured in the same set of experiments.

Fig. S13 Statistical comparison of *ht1-2* mutant and Col-0 wild-type measured at low light condition (LL: 150 μmol m^{-2} s^{-1}) with Col-0 wild-type control measured at high light condition (Col-0: 500 μmol m^{-2} s^{-1}) in the same set of experiments.

Fig. S14 Statistical comparison of *ost1-3* mutant, *ht1-A109V* mutant, and *nced3-2/nced5-2* double mutant and Col-0 wild-type at dark with Col-0 wild-type control measured at high light condition (500 μmol m^{-2} s^{-1}) in the same set of experiments.

Fig. S15 Statistical comparison of *blus1-3* mutant, *ht1-2* mutant, and *cbc1/cbc2* double mutant with Col-0 wild-type control measured in the same set of experiments.

Fig. S16 Statistical comparison of *phyB-9* mutant and *phot1-5/phot2-1* double mutant with Col-0 wild-type control measured in the same set of experiments.

Fig. S17 Statistical comparison of *ht1-A109V* mutant and *mpk12/4-gc-2* double mutant with Col-0 wild-type control measured in the same set of experiments.

Fig. S18 Statistical comparison of stomatal conductance of Col-0 wild-type measured at dark, low light (LL: 150 μmol m^{-2} s^{-1}), and high light (Col-0: 500 μmol m^{-2} s^{-1}) in the same set of experiments.

Fig. S19 Statistical comparison of CO_2 assimilation of Col-0 wild-type measured at dark, low light (LL: 150 μmol m^{-2} s^{-1}), and high light (Col-0: 500 μmol m^{-2} s^{-1}) in the same set of experiments.

Table S1 Primers used in this study.

Please note: Wiley is not responsible for the content or functionality of any Supporting Information supplied by the authors. Any queries (other than missing material) should be directed to the *New Phytologist* Central Office.